*Title Page

A multi-isotopic approach to investigate the influence of land use on nitrate removal in a highly saline lake-aquifer system

N. Valiente[a], R. Carrey[b], N. Otero[b, c], A. Soler[b], D. Sanz[a], A. Muñoz-Martín[d], F. Jirsa[e,f], W. Wanek[g] and J.J. Gómez-Alday[a,*]

a Biotechnology and Natural Resources Section, Institute for Regional Development (IDR), University of Castilla–La Mancha (UCLM), Campus Universitario s/n, 02071 Albacete, Spain

b Grup de Mineralogia Aplicada, Geoquímica i Geomicrobiología, Dept. Mineralogia, Petrologia i Geologia Aplicada, Facultat de Ciències de la Terra, Universitat de Barcelona (UB), C/ Martí i Franquès s/n, 08028, Barcelona, Spain

c Serra Hunter Fellowship, Generalitat de Catalunya, Spain

d Applied Tectonophysics Group, Departamento de Geodinámica, Universidad Complutense de Madrid, C/ José Antonio Novais 2, 28040, Madrid, Spain

e Institute of Inorganic Chemistry, University of Vienna, Althanstrasse 14, 1090 Vienna, Austria

f Department of Zoology, University of Johannesburg, PO Box 524, Auckland Park, 2006, Johannesburg, South Africa

g Division of Terrestrial Ecosystem Research, Department of Microbiology and Ecosystem Science, University of Vienna, Althanstrasse 14, 1090, Vienna, Austria

(*) Corresponding author

*Graphical Abstract

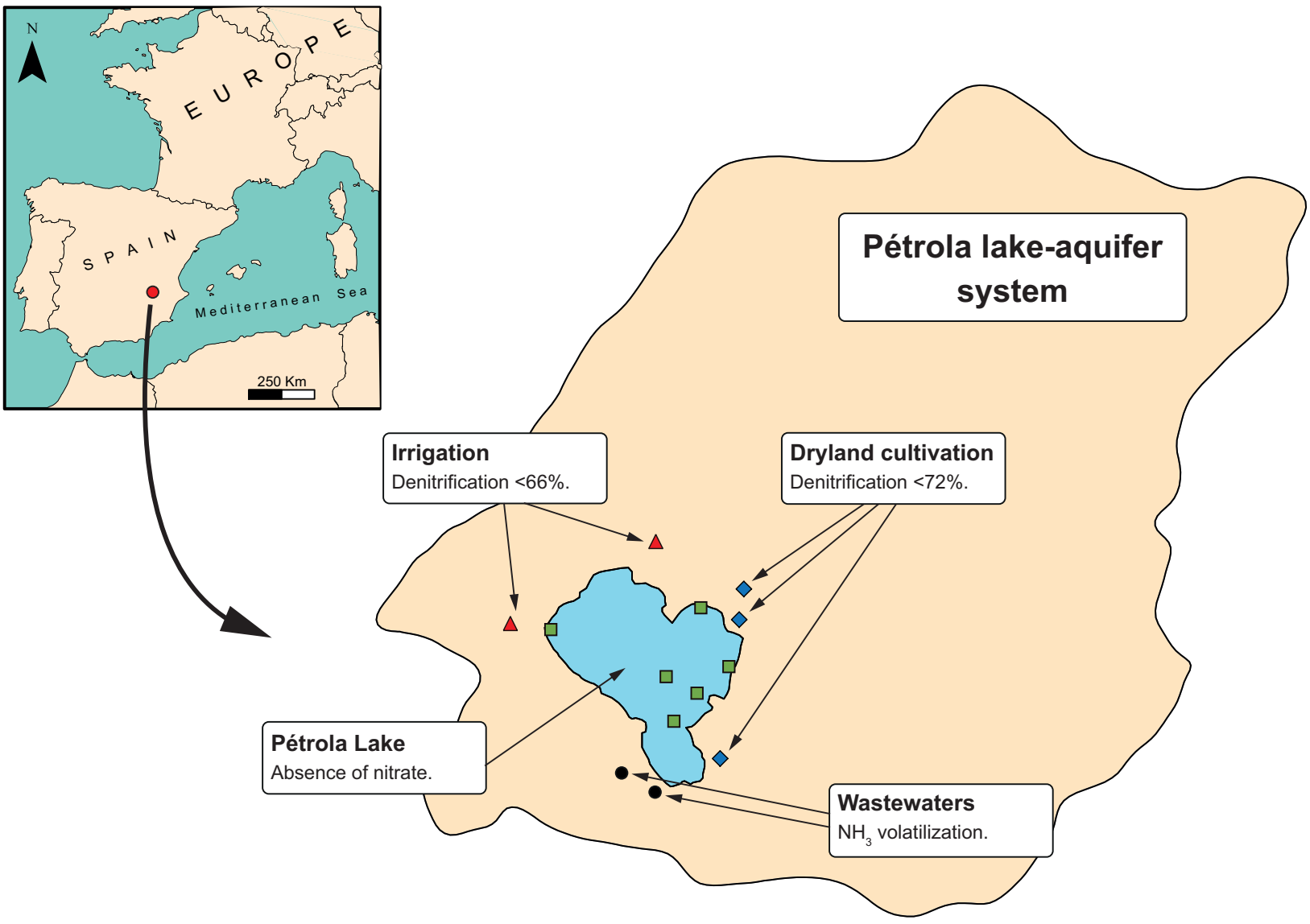

A multi-isotopic approach to investigate the influence of land use on nitrate removal in a highly saline lake-aquifer system

Highlights

Density-driven down flow transports chemicals involved in nitrogen cycling.

Nitrate removal processes are associated to the freshwater-saltwater interface.

The geometry of the freshwater-saltwater interface is influenced by land use.

Natural attenuation of nitrate is mainly linked to agricultural areas.

A multi-isotopic approach to investigate the influence of land use on nitrate removal in a highly saline lake-aquifer system

N. Valiente[a], R. Carrey[b], N. Otero[b, c], A. Soler[b], D. Sanz[a], A. Muñoz-Martín[d], F. Jirsa[e,f], W. Wanek[g] and J.J. Gómez-Alday[a,*]

a Biotechnology and Natural Resources Section, Institute for Regional Development (IDR), University of Castilla–La Mancha (UCLM), Campus Universitario s/n, 02071 Albacete, Spain

b Grup de Mineralogia Aplicada, Geoquímica i Geomicrobiología, Dept. Mineralogia, Petrologia i Geologia Aplicada, Facultat de Ciències de la Terra, Universitat de Barcelona (UB), C/ Martí i Franquès s/n, 08028, Barcelona, Spain

c Serra Hunter Fellowship, Generalitat de Catalunya, Spain

d Applied Tectonophysics Group, Departamento de Geodinámica, Universidad Complutense de Madrid, C/ José Antonio Novais 2, 28040, Madrid, Spain

e Institute of Inorganic Chemistry, University of Vienna, Althanstrasse 14, 1090 Vienna, Austria

f Department of Zoology, University of Johannesburg, PO Box 524, Auckland Park, 2006, Johannesburg, South Africa

g Division of Terrestrial Ecosystem Research, Department of Microbiology and Ecosystem Science, University of Vienna, Althanstrasse 14, 1090, Vienna, Austria

(*) Corresponding author

Abstract

Endorheic or closed drainage basins in arid and semi-arid regions are vulnerable to pollution. Nonetheless, in the freshwater-saltwater interface of endorheic saline lakes, oxidation-reduction (redox) reactions can attenuate pollutants such as nitrate (NO_3^-). This study traces the ways of nitrogen (N) removal in the Pétrola lake-aquifer system (central Spain), an endorheic basin contaminated with NO_3^- (up to 99.2 mg/L in groundwater). This basin was declared vulnerable to NO_3^- pollution in 1998 due to the high anthropogenic pressures (mainly agriculture and wastewaters). Hydrochemical, multi-isotopic ($\delta^{18}O_{NO3}$, $\delta^{15}N_{NO3}$, $\delta^{13}C_{DIC}$, $\delta^{18}O_{H2O}$, and $\delta^{2}H_{H2O}$) and geophysical techniques (electrical resistivity tomography) were applied to identify the main redox processes at the freshwater-saltwater interface. The results showed that the geometry of this interface is influenced by land use, causing spatial variability of nitrogen biogeochemical processes over the basin. In the underlying aquifer, NO_3^- showed an average concentration of 38.5 mg/L (n=73) and was mainly derived from agricultural inputs. Natural attenuation of NO_3^- was observed in dryland farming areas (up to 72%) and in irrigation areas (up to 66%). In the Pétrola Lake, mineralization and organic matter degradation in lake sediment play an important role in NO_3^- reduction. Our findings are a major step forward in understanding freshwater-saltwater interfaces as reactive zones for NO_3^- attenuation. We further emphasize the importance of including a land use perspective when studying water quality-environmental relationships in hydrogeological systems dominated by density-driven circulation.

Keywords

Biogeochemical cycles

Groundwater

Land use

Nitrate attenuation

Stable isotopes

Variable density

1. Introduction

Saline lakes have an important geochemical influence on water resources, ecological dynamics, and economic activities around the world (Jones and Deocampo, 2003). The volume of inland saline waters worldwide (about 104,000 km^3) is similar to the volume of freshwaters (Williams, 1996). Saline wetlands are mostly located in arid and semi-arid regions associated to endorheic basins, since these basins are closed drainage areas with no outlet other than evaporation (Eugster and Hardie, 1978; Yechieli and Wood, 2002). At the same time, these are environments highly vulnerable to pollution due to their low precipitation and high evaporation rates (Schütt, 1998).

The understanding of freshwater-saltwater interfaces in saline wetlands is important to comprehend shallow hydrogeological processes (Cartwright et al., 2009). Physical and biogeochemical processes control the chemical evolution of lakes and the groundwater of the connected aquifer (Castanier et al., 1993; Güler and Thyne, 2004; Skidmore et al., 2010). Solutes can enter into lakes through precipitation, surface runoff (e.g. irrigation returns and wastewater spills) and groundwater. In saline lakes, solutes also can be transported by density-driven flow (DDF) from the surface lake water to deep zones of the aquifer through the freshwater-saltwater interface (Wood and Sanford, 1990; Avrahamov et al., 2014; Colombani et al., 2015).

Andersen et al., (2005) and Santoro (2010), among others, have shown that the freshwater-saltwater interface in estuarine and coastal environments is a favorable area for oxidation-reduction (redox) reactions using organic carbon as electron donor, but little is known on the biogeochemical functions of this interface in saline inland lake systems. In aquatic environments, the redox

reactions follow a sequence based on thermodynamic principles that may also follow temperature gradients (Stumm and Morgan, 1981; Orozco-Durán et al., 2015; Daesslé et al., 2017). There are, however, also contradictory findings on this redox sequence as the reduction of different electron acceptors may occur simultaneously (Postma and Jakobsen, 1996).

NO_3^- is one of the main pollutants affecting surface and groundwater due to its negative effects on human health (Fraser, 1981; Gulis et al., 2002) and on the environment. It causes eutrophication of inland waters (Ryther and Dunstan, 1971; Smith, 1998). Under anaerobic conditions, NO_3^- can be reduced through microbial processes. The main natural attenuation process in aquatic environments is denitrification, which is mainly limited by the electron donors' availability (Korom, 1992; Rivett et al., 2008). Denitrifiers can obtain metabolic energy from: i) oxidation of organic compounds (chemoorganotrophic heterotrophs), or ii) oxidation of inorganic compounds (chemolithotrophic autotrophs). Heterotrophic denitrification is linked to organic matter oxidation (Eq. 1), whereas autotrophic denitrification is related to the oxidation of reduced such as inorganic sulfur compounds (Eq. 2).

$$5CH_3COO^- + 8NO_3^- + 8H^+ \rightarrow 4N_2 + 5HCO_3^- + 5CO_2 + 9H_2O \qquad \text{(Eq. 1)}$$

$$5FeS_2 + 14NO_3^- + 4H^+ \rightarrow 7N_2 + 10SO_4^{2-} + 5Fe^{2+} + 2H_2O \qquad \text{(Eq. 2)}$$

In aquatic environments, NO_3^- can be also affected by other processes such as dissimilatory nitrate reduction to ammonium (DNRA) (Burgin and Hamilton, 2007). DNRA involves the transformation of NO_3^- to ammonium (NH_4^+) both by

heterotrophic organisms, which use organic carbon as the electron donor (fermentative DNRA) (Eq. 3), and by chemolithoautotrophic organisms, which use nitrate to oxidize sulfide or other reduced inorganic substrates (Eq. 4).

$$CH_3COO^- + NO_3^- + 2H^+ \rightarrow NH_4^+ + HCO_3^- + CO_2 \quad \text{(Eq. 3)}$$

$$3FeS_2 + 8NO_3^- + 32H^+ \rightarrow 8\ NH_4^+ + 6SO_4^{2-} + 3Fe^{2+} \quad \text{(Eq. 4)}$$

Contrary to denitrifying bacteria, fermentative bacteria responsible for DNRA are strict anaerobes (Hill, 1996). Heterotrophic DNRA seems to be promoted when NO_3^- is limited and organic carbon is in excess, whereas denitrification is the dominant process when organic carbon is the constraining factor (Tiedje, 1988; Korom, 1992; Kelso et al., 1997). The prevalence of one or the other can be predicted by the organic C:N ratio of available substrates (Tiedje, 1982; Kraft et al., 2011; van den Berg et al., 2016). Prior studies suggested that DNRA may be as important, if not more dominant, than denitrification as a sink for NO_3^- in reducing environments with high sulfide contents (Brunet and Garcia-Gil, 1996; Trimmer et al., 1998). The available research recognizes the role of other microbial processes that remove NO_3^- in aquatic ecosystems, such as anaerobic ammonium oxidation (Anammox; Jetten et al., 1998) and NO_3^- reduction coupled to iron and manganese oxidation (Postma et al., 1991; Weber et al., 2006).

The analysis of stable isotopes coupled to hydrochemical investigations is a widely accepted approach to understand biogeochemical processes in groundwater. Multi-isotopic analyses have been applied to elucidate NO_3^-

127 sources (Vitòria et al., 2004; Kendall et al., 2007) as well as to trace major
128 biogeochemical cycles and their related bacterial-mediated redox reactions in
129 aquifers and surface water systems (Jurado et al., 2013; Puig et al., 2013;
130 Hosono et al., 2014; Caschetto et al., 2017).

131 The Pétrola endorheic basin, which was declared a nature reserve in 2005
132 (Spanish Decree 102/2005, September 13th), is located in a zone vulnerable to
133 NO_3^- pollution, where fertilizer use is restricted since April 2011 (Order 2011/7/2
134 CMA). Previous studies have shown the potential of sediments in the Pétrola
135 basin to promote NO_3^- attenuation at the laboratory scale (Carrey et al., 2013,
136 2014a, 2014b). Gómez-Alday et al. (2014) confirmed heterotrophic
137 denitrification at the field scale, where density-driven flow from surface lake
138 waters towards the underlying aquifer played an important role in solute
139 transport. Nonetheless, the main NO_3^- reduction pathway in the Pétrola Lake
140 remains unknown (Valiente et al., 2016). Previous studies in the Pétrola basin
141 (Valiente et al., 2017) highlighted the importance of bacterial sulfate-reduction
142 (BSR) processes in lake sediments and groundwater below the lake. These
143 BSR processes were carried out, among others, by *Desulfovibrio* spp., which
144 have also been identified as being responsible for dissimilatory NO_3^- reduction
145 to NH_4^+ (McCready et al., 1983).

146 The goal of this paper was to identify the unusual ways of nitrogen removal in
147 the Pétrola saline lake-aquifer system as an example of natural biodegradation
148 of NO_3^- at the freshwater-saltwater interface. The effects of anthropogenic
149 pressure on geochemical processes and solute transport may be extrapolated
150 to other systems dominated by density-driven circulation around the world. To
151 that end, hydrochemical, multi-isotopic and geophysical techniques were

152 applied to trace the redox processes in the Pétrola basin. Hydrochemical and
153 multi-isotopic techniques are highly suitable to trace pollution sources while
154 geophysical tools may help to understand the geometry of the freshwater-
155 saltwater interface.

156

157 ***2. Study area***

158 The Pétrola Endorheic Basin (PEB) is located in the High Segura River Basin,
159 in central Spain (Figure 1). The High Segura River Basin includes an important
160 saline endorheic complex named the Pétrola–Corral-Rubio–La Higuera Saline
161 Complex (about 275 km^2), with a total of 19 wetlands (Cirujano et al., 1988).
162 The main wetland of the complex is the Pétrola lake, with an area of 43 km^2.
163 The climate of the study area is Mediterranean, continental, and semi-arid, with
164 mean annual precipitation below 400 mm, predominantly falling during spring
165 and autumn. The average monthly temperatures vary from 4.9 ºC in January to
166 24.2 ºC in July and the mean annual temperature is 14.3 °C.

167 ---------- Fig. 1 near here ----------

168 Geologically, the study area consists mainly of Mesozoic materials. The base of
169 the Lower Cretaceous unit reaches the Barremian and consists of argillaceous
170 sediments overlain by sands and sandy-conglomerate sediments with
171 intergranular porosity (Weald Facies). Aptian carbonates cover Barremian
172 terrigenous deposits. The Utrillas Facies are Albian deposits composed of
173 siliciclastic sands, sandy conglomerates, and reddish to dark-grey clay to
174 argillaceous sediments deposited over Aptian sediments. The Utrillas sediments
175 include sandy-conglomerate sediments interstratified by grey-to-black

176 argillaceous sediments. These sediments are rich in organic matter and sulfides
177 (mainly pyrite), composing the main part of the aquifer. Sulfides from the Lower
178 Cretaceous sediments are oxidized to gypsum by weathering processes
179 (Gómez-Alday et al., 2004). The piezometric level of the Cretaceous aquifer is
180 close to the topographic surface. Consequently, several springs and streams
181 drain the aquifer in this area. The lake acts as a discharge zone for these water
182 flows, which follow a radial pattern towards the lake. Previous research has
183 shown that the Pétrola lake-aquifer system shows two main flow components:
184 regional groundwater flow (RGF, up to 1.01 g/cm^3) from recharge areas to the
185 lake, and a density-driven flow (DDF, up to 1.29 g/cm^3) from surface water to
186 the underlying aquifer (Gómez-Alday et al., 2014; Valiente et al., 2017).

187 The catchment area of the Pétrola lake-aquifer system supports agricultural and
188 livestock activities. Two types of farming are present: dryland farming and
189 irrigation farming (Figure 1). Farming encompasses approximately 75% of the
190 total area, whereby dryland farming contributes about 58% and irrigated
191 cropland 17%, based on data from Corine Land Cover 2012 (Soukup et al.,
192 2016). The remaining area is occupied by semi-natural land cover types, such
193 as Mediterranean forest and scrubland (19%). The use of inorganic synthetic
194 fertilizers is the main source of pollutant N in the system. The estimated N load
195 produced by agricultural activities was about 10 t/km^2 year^{-1} (year 2000) (ITAP,
196 2010), in the range of other studies in lake catchments and wetlands worldwide
197 (Saunders and Kalff, 2001).

198

3. Material and methods

3.1. Sampling

Between March 2013 and July 2015, a total of 119 water samples were collected from 13 control points located in the Pétrola Lake and near the lake discharge area, following the groundwater flow direction (including springs and streams). Hereafter, this zone will be referred as surrounding area. The sample points were distributed in 4 subzones according to the main anthropogenic pressure and location: surface lake water samples (Group 1: sites 2635, 2643, 2648, 2649, 2651 and 2652), wastewaters (Group 2: sites 2575 and 2641), dry farming area (Group 3: sites 2554, 2640 and 2642) and irrigation area (Group 4: sites 2571 and 2602). The latter three subzones are located in the surrounding area of the lake (Figure 1).

In addition, between September 2014 and July 2015, 13 sediment cores, 5 cm in depth, were collected from the bottom of the lake using Plexiglas cylinders. The locations for sampling correspond to control points 2648, 2649, 2651 and 2652. The cores were frozen at -20 ºC and freeze-dried for further analysis. Groundwater levels were measured using a ceramic CTD-Diver stand-alone sensor installed in a PVC piezometer (GW-12) at 6 meters below ground surface (mbgs). This piezometer was installed near control point 2635. Thus, the groundwater level at GW-12 is closely related to the Pétrola Lake water level and is influenced by precipitation (Gómez-Alday et al., 2014). Groundwater level data were collected from January 2012 to February 2015, with logging intervals of 24 h (n=1,151 daily measurements). Precipitation data for the study period were gathered from the meteorological station AB07 (Ministry of

223 Agriculture and Fisheries, Food and Environment of Spain) situated in Pozo
224 Cañada village, about 16 km SW from Pétrola Lake.

225

226 ***3.2. Chemical and isotopic analyses***

227 In all water samples immediately after sample collection temperature (T), pH,
228 electrical conductivity (EC), total dissolved solids (TDS), redox potential (Eh)
229 and dissolved oxygen (DO) were measured (n=110) *in situ* using a HQ40d
230 Portable Multi-Parameter Meter (Hach Company, USA). Accuracy of physico-
231 chemical determinations was ± 0.3 ºC for T, ± 0.002 for pH, ± 0.5% for EC and
232 TDS (<200 mS/cm), ± 0.1 mV for Eh, and ± 0.01 mg/L for DO.

233 Water samples were stored at 4 °C in a dark environment for subsequent
234 analyses. Alkalinity (HCO_3^- and CO_3^{2-}) was determined by titration in the
235 laboratory following standard methods (APHA-AWWA-WEF, 1998), with a limit
236 of detection of 1 mg/L and an accuracy of ± 0.2%. Water samples for major ions
237 and dissolved organic carbon (DOC) were filtered with a 0.20 µm nylon
238 Millipore® filter. DOC concentration was determined by the high temperature
239 combustion method using a Shimadzu TOC-V Analyzer at the Institute of
240 Inorganic Chemistry of the University of Vienna and in the research facilities at
241 the University of A Coruña, with a detection limit of 0.05 mg/L and a
242 reproducibility of ± 1.5%. The concentration of NO_3^- was determined by UV-VIS
243 spectrophotometry following the Griess reaction assay by cadmium reduction to
244 nitrite (NO_2^-) (Wood et al., 1967). The detection limit of NO_3^- measurements was
245 0.3 mg/L. NH_4^+ contents were determined by distillation and volumetric methods
246 (Koroleff, 1969), with a detection limit of 0.02 mg/L. Accuracy for NO_3^- and NH_4^+
247 determinations was ± 1.0%.

The aqueous concentration of Cl^- and SO_4^{2-} was obtained by capillary electrophoresis (CE) using a Waters Quanta 4000 system coupled with a negative power supply and an indirect UV detection system. For Cl^- and SO_4^2 determinations, the limit of detection was 1 mg/L. The methodology for separation and measurement by CE is described in Santoyo et al. (2001). Concentrations of K^+, Na^+, Ca^{2+}, Mg^{2+}, Fe^{2+} and Mn^{2+} were determined combining CE and ICP-AES, with limits of detection of 1 mg/L (K^+, Na^+, Ca^{2+} and Mg^{2+}) and 20 µg/L (Fe^{2+} and Mn^{2+}). Analyses by CE and ICP-AES were performed in the research facilities at the National Museum of Natural History (Madrid, Spain), with accuracy values of ± 1.0%.

The isotopic analyses included the $\delta^{15}N$ and $\delta^{18}O$ of NO_3^-, $\delta^{13}C$ of DIC, and δ^2H and $\delta^{18}O$ of H_2O. The $\delta^{15}N_{NO3}$ and $\delta^{18}O_{NO3}$ were measured using a Cd-reduction method (McIlvin and Altabet, 2005, Ryabenko et al., 2009). Briefly, NO_3^- was converted to NO_2^- through spongy cadmium reduction and then to nitrous oxide using sodium azide in an acetic acid buffer. Simultaneous $\delta^{15}N$ and $\delta^{18}O$ analysis of the N_2O produced was carried out using a Pre-Con (Thermo Scientific) coupled to a Finnigan MAT-253 Isotope Ratio Mass Spectrometer (IRMS, Thermo Scientific). The $\delta^{13}C_{DIC}$ was determined from filtered water samples, which were treated with ortho-phosphoric acid and shaken for at least 2 hours in order to convert all bicarbonate into CO_2 and reach equilibrium between aqueous and gaseous phases, and the isotope ratio was measured in a Gas-Bench II coupled to a MAT-253 IRMS (Thermo Scientific). The δ^2H_{H2O} and $\delta^{18}O_{H2O}$ were measured using H_2 and CO_2 equilibrium techniques, respectively, following standard methods (Epstein and

Mayeda, 1953). $\delta^{2}H_{H2O}$ and $\delta^{18}O_{H2O}$ were measured by dual inlet IRMS on a Finnigan MAT Delta S.

Results are expressed in δ (‰) values relative to international standards Vienna Pee Dee Belemnite (V-PDB) for $\delta^{13}C$, atmospheric N_2 (AIR) for $\delta^{15}N$, and Vienna Standard Mean Ocean Water (V-SMOW) for $\delta^{18}O$ and $\delta^{2}H$. Analytical reproducibility by repeated analysis of both international and internal reference samples of known isotopic composition was ± 0.3‰ for $\delta^{13}C_{DIC}$, ± 0.3‰ for $\delta^{15}N_{NO3}$, ± 0.5‰ for $\delta^{18}O_{NO3}$, ± 1‰ for $\delta^{2}H_{H2O}$, and ± 0.3‰ for $\delta^{18}O_{H2O}$. Samples for isotope analyses (n=119) were prepared at the laboratory of the Mineralogia Aplicada i Geoquimica de Fluids research group (Universitat de Barcelona). Isotope analyses were performed at the Centres Cientific Tècnis of Universitat de Barcelona.

In sediment samples (n=13), organic matter content was determined as loss on ignition (LOI) by combustion of dried sediment for 2 h at 550 °C in a muffle furnace at the Institute of Inorganic Chemistry of the University of Vienna, following Nelson and Sommers (1996). The method has a detection limit of 0.05%. Elemental Analysis was performed to determine the percentage of total carbon (TC), soil organic carbon (SOC), and total nitrogen (TN). In addition, $\delta^{13}C$ in TC and SOC, and $\delta^{15}N$ in TN from lake sediment samples were determined. For this purpose, the samples were dried and finely ground. Samples were acidified with concentrated HCl and vacuum-dried overnight before analysis of organic carbon content. The parameters were measured on untreated and acidified sediment samples using an elemental analyzer (EA 1110 CE Instruments) coupled to a DELTA^{plus} IRMS (Finnigan MAT) in the SILVER Lab, University of Vienna. C:N ratios were calculated as the ratio of

297 SOC and TN. Reproducibility using soil standards was ± 0.1‰ for $\delta^{13}C$, and ±
298 0.15‰ for $\delta^{15}N$.

299

300 ***3.3. Electrical Resistivity Tomography (ERT)***

301 The ERT survey was performed to investigate the geometry of the DDF in the
302 lake discharge area. It was carried out in June 2012 using a RESECS DMT
303 resistivity meter equipped with 72 electrodes. The electrode configuration was a
304 Wenner array, in order to reach the highest signal-to-noise ratio (SNR) and
305 sensitivity to vertical variations in resistivity (Loke and Dahlin, 2002). Electrode
306 spacing values were 2.5 m (ERT profiles A, D and E) and 5 m (ERT profiles B
307 and C). Twenty-three research levels were considered, to reach 60 m depth in
308 the central part of each section. At each measurement section, two injection
309 cycles were applied, recording 700 electric potential differences and intensity
310 values, and calculating the Root Mean Square (RMS) error for each apparent
311 resistivity value.

312 Five sections were measured following a radial pattern, from the lake's margins
313 to about 350 m far into the basin (Figure 1). Locations were selected based on
314 streams and springs with potential NO_3^- inputs to the lake. The first profile, ERT-
315 A, was 315 m long and was set up along an irrigated cropland. ERT-B was
316 parallel to a stream (control point 2571) and was about 350 m long. ERT-C,
317 about 155 m in length, was situated at the east side of the lake, with control
318 point 2648 as final point. ERT-D, 235 m long, extended from the lake's margin
319 to control point 2602. Finally, ERT-E (175 m in length) started from the lake
320 shore towards control point 2641, passing close to control point 2575. Individual
321 measurement points were revised taking into account standard deviation, RMS,

322 and spontaneous potential. All values with a standard deviation higher than
323 20% were removed in order to improve signal/noise ratio. Field data inversion
324 was performed with Res2Dinv software using the same parameters in the
325 inversion for all ERT profiles (deGroot-Hedlin and Constable, 1990; Loke and
326 Barker, 1996). For inversion, a least-squares inversion algorithm was chosen.
327 Final calculated RMS errors for the five sections ranged between 7.4% (ERT-E)
328 and 15.8% (ERT-B). Inversion results were exported to absolute XYZ
329 coordinates in order to compare them with hydrogeological and geochemical
330 data.

331

332 ***4. Results***

333 ***4.1. Hydrochemical data***

334 Chemical data for water samples from the four groups are presented in the
335 Supplementary Information (Appendix A). Lake water samples (Group 1) had a
336 mean pH value of 8.6 and a maximum of 9.4. Eh values were between -227 mV
337 and +451 mV. Dissolved oxygen (DO) values ranged from 0.2 to 13.0 mg/L.
338 Values of EC and TDS peaked at 83,600 µS/cm and 50 g/L, respectively.
339 Dissolved Organic Carbon (DOC) concentrations varied between 24.5 mg/L and
340 289.2 mg/L. NO_3^- concentrations in most of the samples were below detection
341 limit (<0.3 mg/L), reaching values up to 1.2 mg/L. NH_4^+ concentrations ranged
342 from below detection limit (<0.02 mg/L) to 6.5 mg/L. The concentrations of
343 SO_4^{2-} and Cl^- ranged from minimum values of 4,683 mg/L and 3,253 mg/L,
344 respectively, to maximum values of 40,678 mg/L and 29,099 mg/L, respectively.
345 HCO_3^- concentrations varied between 178 and 507 mg/L, the CO_3^{2-}
346 concentration from 2.3 to 45.9 mg/L. Peak Fe^{2+} and Mn^{2+} concentrations were

104 µg/L and 400 µg/L, respectively. Nevertheless, a significant percentage of the samples showed Fe^{2+} and Mn^{2+} concentrations below the detection limit (<20 µg/L). Overall the hydrofacies of the lake water can be classified as Mg-Na-SO_4-Cl (6 control points, March 2013 to July 2015; n=37) (Figure 2).

---------- Fig. 2 near here ----------

The groundwater samples of the surrounding area (groups 2, 3 and 4) had pH values of 7.3-8.8. Eh ranged from -192 mV to +484 mV, DO values from 0.2-19.6 mg/L. EC and TDS values ranged from 975-2,820 µS/cm, and from 0.5-1.5 g/L, respectively. DOC concentrations ranged from 1.3-22.7 mg/L. NO_3^- concentrations ranged from below detection limit to 99.2 mg/L. NH_4^+ concentrations varied from 0.1 to 43.0 mg/L, SO_4^{2-} from 139-1,091 mg/L, Cl^- from 88-484 mg/L. HCO_3^- concentrations ranged from 249-769 mg/L, CO_3^{2-} from 0.4-13.3 mg/L. Fe^{2+} and Mn^{2+} concentrations were mainly below the detection limit, reaching values of up to 43 µg Fe^{2+}/L and 888 µg Mn^{2+}/L, respectively. The groundwater type in the surrounding area varied between Mg-Ca-SO_4-HCO_3 and Na-Ca-HCO_3-Cl, as shown in Figure 2 (7 control points, March 2013 to July 2015; n=73).

4.2. Isotope data in water samples

The complete record of isotope data in water samples is included in the Supplementary Information (Appendix B). For Group 1 samples (Pétrola Lake), δ^2H_{H2O} varied from -48.2‰ to +35.4‰ (average +5.8‰; n=40), whereas $\delta^{18}O_{H2O}$ ranged between -6.7‰ and +11.0‰ (average +1.7‰; n=40). $\delta^{15}N_{NO3}$ and $\delta^{18}O_{NO3}$ were not determined for lake samples due to the low NO_3^-

concentrations measured. $\delta^{13}C_{DIC}$ values varied between -16.3‰ and -4.8‰ (average of -8.7‰; n=40). In samples from the surrounding area (Groups 2, 3 and 4), $\delta^{2}H_{H2O}$ and $\delta^{18}O_{H2O}$ varied between -55.1‰ and -12.8‰ and between -8.7‰ and -+0.7‰, respectively. $\delta^{15}N_{NO3}$ signatures ranged from +6.6‰ to +21.6‰ and $\delta^{18}O_{NO3}$ from +1.5‰ to +16.9‰. $\delta^{13}C_{DIC}$ values ranged between -14.3‰ and -6.4‰ (average -10.8‰; n=79).

4.3. Sediment data

The full data record is included in Supplementary Information (Appendix C). LOI values ranged from 3.1% to 19.0% (average of 7.2%; n=13). The contents of TC and SOC, ranged from 2.41% to 13.2% (average 5.70%; n=13) and from 0.68% to 6.10% (average 2.65%; n=13), respectively. $\delta^{13}C$ in TC and SOC ranged from -14.6‰ to -2.3‰ (average -8.6‰; n=13) and from -25.1‰ to -3.1‰ (average -13.0‰; n=13), respectively. TN varied between 0.04% and 0.62% (average 0.18%; n=13) and $\delta^{15}N_{TN}$ between +9.2‰ and +14.4‰ (average +10.6‰; n=13). C:N ratios varied between 4.4 and 57.3, with a mean value of 23.0 (n=13).

4.4. Groundwater level and ERT data

Between May and October 2012, the groundwater level gradually fell in GW-12, concurring with a very low precipitation period (Figure 3). Heavy rainfalls in autumn 2012 increased the groundwater level, which peaked in March 2013. From January 2013 to May 2014, frequent rainfall sustained groundwater level depths between 0.15 mbgs and 0.45 mbgs. Little precipitation during spring and

summer 2014 caused the groundwater level to fall again, reaching a maximum depth of 1.43 mbgs on 31 October 2014. Concurring with major precipitation events during winter 2014 and spring 2015, the groundwater level increased from November 2014 to the final recording.

The ERT survey was conducted in June 2012 and showed a resistivity distribution related to several parameters such as water content, porosity and EC. A complete description of ERT profiles is included in Supplementary Information (Appendix D).

---------- Fig. 3 near here ----------

5. Discussion

5.1. Hydrogeochemical and isotopic ($\delta^{18}O_{H2O}$ and $\delta^{2}H_{H2O}$) evolution of the lake water

ERT profiles A, B, C and E demonstrated a salt-water wedge located around the lake, indicating the influence of Pétrola Lake on groundwater (Figure 4). Water samples from the surrounding area are characterized by low EC values (<2,820 µS/cm) compared to lake waters. ERT-A showed a layer of high resistivity that swelled to the NNW due to the presence of irrigation return flows. ERT-B was conducted through a zone with both irrigation and dryland conditions, pointing to the presence of a saline wedge under site 2571. ERT-C was performed in an area with no irrigation (dryland, Group 3) but very close to the lake. The influence of Pétrola Lake on samples from Group 2 (wastewaters) was observed in ERT-E. Resistivity values throughout this profile had intermediate values, showing a limited influence of freshwaters. ERT-D was

419 also performed in an area with both irrigation and dryland conditions. This
420 profile is explained by the influence of irrigation return flows causing an influx of
421 low salinity (high resistivity) water into the aquifer, contrary to what would be
422 expected when solute transportation occurs from the lake to the Cretaceous
423 aquifer. In general, the observed heterogeneity of the freshwater-saltwater
424 interface can be explained by the different land uses at the basin scale. Our
425 results suggest that the saline wedge can be displaced by less dense
426 groundwater in those regions of the aquifer where the influence of irrigation
427 return flows was significant. The saline wedge is shifted towards areas with less
428 influence of irrigation (SE of the basin) favored by the compression of the
429 upward component of the RGF.

430 Other than land use, the effect of climatic conditions on lake and aquifer
431 hydrochemistry must also be considered. During periods with low precipitation,
432 the groundwater level in GW-12 fell. Simultaneously, TDS values increased in
433 lake water as result of both evaporation and solute concentration (Figure 3).
434 Consequently, the highest concentrations of Cl^-, SO_4^{2-} and Mg^{2+} in lake water
435 are expected during periods of lowest water level in GW-12, leading to a Mg-
436 Na-SO_4-Cl water type during dry periods (Valiente et al., 2017). These
437 conditions are favorable for DDF to transport solutes from the lake into deeper
438 aquifer zones. Thus, changes in the water chemistry of lake samples were
439 reflected in groundwater hydrochemistry. In the lake, DOC derived mainly from
440 autochthonous (primary productivity) and allochthonous (wastewaters) sources
441 (Gómez-Alday et al., 2014). Lake water samples showed increasing DOC
442 concentrations during low precipitation periods (up to 289.2 mg/L), which may
443 be transported from the lake to the aquifer by DDF. This caused a flux of DOC

444 across the freshwater-saltwater interface, fueling microbial processes in deeper
445 aquifer zones.

446 The $\delta^{18}O_{H2O}$ and $\delta^{2}H_{H2O}$ in water samples showed the influence of precipitation
447 and evaporation processes on the lake-aquifer system (Figure 4). Samples from
448 PEB were compared with the local meteoric water line of Madrid (LMWL), its
449 weighted isotopic composition of monthly average precipitation, and the
450 regression line for $\delta^{18}O_{H2O}$ and $\delta^{2}H_{H2O}$ values in water samples between 2008
451 and 2010 (Valiente et al., 2017). Madrid was selected as a reference station
452 because most of the rainfall events in the study area are influenced by
453 European Atlantic fronts, which are also dominant in Madrid. Evaporation
454 processes can be inferred from the slope of plots of $\delta^{18}O_{H2O}$ and $\delta^{2}H_{H2O}$ isotopic
455 compositions of evaporating water bodies. This is because of the similar kinetic
456 isotope enrichment in ^{18}O and ^{2}H during evaporation in dry air, whereas the
457 equilibrium isotope fractionation during condensation differs between hydrogen
458 and oxygen by a factor of 8. Therefore, evaporation of rainwater causes a
459 decrease in the slope of the $\delta^{18}O_{H2O}$ and $\delta^{2}H_{H2O}$ plots, from 8‰ towards ~3‰
460 (Clark and Fritz, 1997). The $\delta^{18}O_{H2O}$ and $\delta^{2}H_{H2O}$ values from lake samples did
461 not remain constant during the period March 2013 to July 2015 (Figure 4),
462 showing a mean and standard deviation for $\delta^{18}O_{H2O}$ and $\delta^{2}H_{H2O}$ in measured
463 samples of +1.7‰ ±4.8‰ and -5.8‰ ± 23.1‰, respectively. Lake samples
464 showed a slope of 4.7 for $\delta^{18}O_{H2O}$ and $\delta^{2}H_{H2O}$ values (R^2=0.98; n=40), a typical
465 slope for evaporation. This slope was significantly lower than the LMWL (6.8)
466 and only slightly lower than the slope of water samples from previous studies
467 (5.2 between 2008 and 2010; Valiente et al., 2017).

468 ---------- Fig. 4 near here ----------

469 The influence of the lake on control points of the surrounding area was also
470 evident: $\delta^{18}O_{H2O}$ and $\delta^{2}H_{H2O}$ values here were enriched with reference to the
471 weighted average precipitation ($\delta^{18}O_{H2O}$= -7.0‰, $\delta^{2}H_{H2O}$= -47.8‰). Water
472 samples close to the weighted average precipitation value showed the influence
473 of regional groundwater and a lesser influence of the Pétrola Lake. In contrast,
474 samples collected in April 2015 from Group 2, Group 3 (except control point
475 2554) and Group 4 followed a mixing line from meteoric water to lake waters. At
476 this date, control point 2635 showed $\delta^{18}O_{H2O}$ and $\delta^{2}H_{H2O}$ values of +1.5‰ and -
477 2.7‰, respectively. These findings are in agreement with ERT profiles, showing
478 the influence of lake waters on sites of Group 2 (ERT-E) and Group 4 (ERT-B).

479

480 ***5.2. Nitrogen recycling in the lake-aquifer system***

481 Figure 5 shows the $\delta^{15}N_{NO3}$ and $\delta^{18}O_{NO3}$ values in water samples from the
482 surrounding area together with the range of potential NO_3^- sources in PEB
483 (adapted from Puig et al. (2016) and references therein). $\delta^{18}O_{NO3}$ values
484 deriving from nitrification of ammonium fertilizers and sewage/manure (from
485 +2.1‰ to +7.4‰) were calculated according to Mayer et al. (2001) with the
486 following expression (Eq. 5):

487 $$\delta^{18}O = 2/3 \cdot \delta^{18}O_{H2O} + 1/3 \cdot \delta^{18}O_{O2} \qquad \text{(Eq. 5)}$$

488 where $\delta^{18}O_{H2O}$ includes the range of values for groundwater in samples from
489 the surrounding area (-8.7‰ and -0.7‰) and $\delta^{18}O_{O2}$ is the isotopic composition
490 of atmospheric O_2 (+23.5‰; Horibe et al., 1973).

491 ---------- Fig. 5 near here ----------

Only two samples from 2575 (influenced by wastewaters) had a high enough NO_3^- concentration to be isotopically characterized. Those two samples showed the lowest NH_4^+ concentrations, and the variability in isotopic composition can be explained by partial nitrification under surface conditions. Water samples (n=10) from site 2641 (close to 2575) showed $\delta^{15}N_{NO3}$ and $\delta^{18}O_{NO3}$ values clearly in the range of manure and sewage. These results reflect the influence of wastewaters at control points 2575 and 2641, with strong nitrogen isotope enrichment due to NH_3 volatilization (Figure 5).

Three samples from Group 3 (dryland cultivation, site 2640) were within the range of soil organic N (between +3‰ and +8‰; Kendall et al., 2007). The origin of NO_3^- for these samples is potentially related to the application of ammonium fertilizers nitrified to NO_3^- in the unsaturated zone. Volatilization and nitrification can produce isotopic signatures of ammonium fertilizers similar to those of soil NO_3^- (Vitòria et al., 2005). The high NO_3^- concentration in samples from site 2640 suggests a contribution from inorganic fertilizers rather than a soil nitrate contribution. The $\delta^{15}N_{NO3}$ and $\delta^{18}O_{NO3}$ values did not negate a potential contribution of nitrate fertilizers, even though no samples fell in the range defined by this type of fertilizers (-4‰ to +8‰ for $\delta^{15}N$ and +17‰ to +25‰ for $\delta^{18}O$; Vitòria et al., 2004). Samples from site 2640 showed a mixing line between the isotopic composition of fertilizer NO_3^- and fertilizer NH_4^+. The contribution of NO_3^- fertilizers can be further masked by the mineralization-immobilization-turnover (MIT) process (Mengis et al., 2001), which can shift the oxygen isotopic composition of NO_3^- fertilizers. During the MIT process, N-NO_3^- is immobilized in the form of organic nitrogen by microbes, subsequently converted to inorganic NH_4^+ by nitrogen mineralization, and finally NH_4^+ is

517 nitrified to NO_3^-. This process changes the oxygen isotope signatures from
518 fertilizer-like to soil nitrification-related.

519 Samples from control points 2554 and 2642, also in Group 3, showed a different
520 trend, with both $\delta^{15}N_{NO3}$ and $\delta^{18}O_{NO3}$ increasing. Denitrification probably
521 explains the isotopic values of the two samples. Prior studies have already
522 shown the NO_3^- attenuation potential of organic-rich bottom sediments from
523 Pétrola Lake and sediments from Utrillas Facies, using organic matter as
524 electron donor (Carrey et al., 2013; Gómez-Alday et al., 2014). A slight
525 denitrification line is observed in samples from 2554. Nonetheless, the
526 denitrification line was much clearer in samples from site 2642. In these
527 samples, the highest $\delta^{15}N_{NO3}$ values (up to +21.6‰) were coupled to relatively
528 low NO_3^- concentrations (10.4 mg/L), indicating denitrification. In fact, these
529 samples were fitted to the denitrification line based on Utrillas and recent
530 organic hypersaline sediments (Figure 5).

531 Finally, samples from Group 4 (control points 2571 and 2602), affected by
532 irrigation return flows, also revealed an increasing trend in the $\delta^{15}N_{NO3}$ vs
533 $\delta^{18}O_{NO3}$ plot, showing that denitrification processes were major contributors to
534 NO_3^- attenuation. At control point 2602, all samples followed a denitrification
535 trend starting from NH_4^+ fertilizers (noted as s2 in Figure 5). Some samples
536 from control point 2571 also followed the denitrification trend. A possible
537 explanation for the clear denitrification trend in those samples is that DDF,
538 which is able to transport solutes involved in attenuation processes, has a
539 greater influence in zones affected by irrigation, as shown in the previous
540 section.

Despite the NO_3^- inputs to the lake from streams, groundwater and wastewaters, most of Pétrola Lake water samples showed NO_3^- below detection limit. Concerning the sedimentary N isotope signatures from Pétrola Lake, the mean $\delta^{15}N_{TN}$ value at 5 cm depth (+10.6‰) was well above the NH_4^+ fertilizer range (from -4‰ to +8‰; Vitòria et al., 2004), but within the range of manure and sewage (from +5‰ to +20‰; Aravena and Mayer, 2009). The isotope composition of N in sediments is influenced by the dominant source of N, microbial recycling and lake productivity (Botrel et al., 2014). This effect may be even stronger in saline lakes due to the high productivity of these ecosystems (Hammer, 1981).

Our results are in agreement with previous studies (Heaton, 1986; Kendall et al., 2007), which established a $\delta^{15}N_{TN}$ range from +10‰ to +20‰ for human and animal wastes. Nevertheless, $\delta^{15}N_{TN}$ signatures can be altered by microorganisms through remineralization (Hodell and Schelske, 1998) and/or degradation of organic matter (Lehmann et al., 2002), resulting in an increase of $\delta^{15}N_{TN}$. Furthermore, sedimentary $\delta^{13}C_{SOC}$ and $\delta^{15}N_{TN}$ values showed an inverse relationship (R^2 = 0.74, n=13), which can be attributed to selective removal of C and N compounds during remineralization (Bernasconi et al., 1997). Thus, our results may reflect a mixed source of synthetic N (ammonium) fertilizers and wastewaters.

5.3. Nitrate attenuation processes

Previous studies showed that the natural attenuation of NO_3^- in the lake-aquifer system can be accomplished by heterotrophic denitrification (Gómez-Alday et al., 2014). For these reactions, DOC is necessary as electron donor. In samples

566 from the surrounding area, DOC is derived mainly from organic matter from
567 Utrillas facies, wastewater and organic matter transported from the lake towards
568 the aquifer by DDF. No increase in NH_4^+ concentration was recorded in
569 samples from the surrounding area. Thus, the enrichment in ^{18}O and ^{15}N in
570 those samples can be attributed mainly to denitrification processes. The isotope
571 composition and concentration of NO_3^- can be used to quantify denitrification at
572 the field scale (Böttcher et al., 1990). Nonetheless, plots of $\delta^{15}N_{NO3}$ vs $Ln[NO_3^-]$
573 using all field samples showed no correlation (R^2=0.19), possibly because of
574 processes such as volatilization or mixing between different groundwater flow
575 lines and mixing of multiple sources and sinks, as described in the previous
576 section. However, in the dual isotope plot some samples followed a
577 denitrification trend. Figure 5 shows ε_N:ε_O ratios determined in denitrification
578 experiments using both bottom sediments of Pétrola lake (1.01; Carrey et al.,
579 2014a) and Utrillas sediments (0.96 and 1.14; Carrey et al., 2013). Using the
580 enrichment factors for nitrogen and oxygen from hypersaline sediments from
581 Pétrola Lake (ε_N = -14.7‰; ε_O = -14.5‰) and Utrillas sediments (ε_N = -11.6‰
582 and -15.7‰; ε_O = -12.1‰ and -13.8‰), the percentage of denitrification was
583 calculated following Eq. (6):

584 $$\mathrm{DEN}(\%) = \left[1 - \frac{[\mathrm{NO_3}]_{\mathrm{residual}}}{[\mathrm{NO_3}]_{\mathrm{initial}}}\right] \cdot 100 = \left[1 - \mathrm{e}^{\frac{\delta_{\mathrm{residual}} - \delta_{\mathrm{initial}}}{\varepsilon}}\right] \cdot 100 \qquad \text{(Eq. 6)}$$

585 To quantify denitrification, only the samples with $\delta^{18}O_{NO3}$ values above +8.0‰
586 from groups 3 and 4 were considered (n=50), to ensure they were above the
587 range of volatilization and nitrification. Denitrification has been modeled using
588 two different initial isotopic compositions that reflect the variability in $\delta^{18}O_{NO3}$
589 derived from nitrification. The first assumed initial composition (s1 in Figure 5)

was $\delta^{15}N_{NO3}$ = +7.0‰ and $\delta^{18}O_{NO3}$ = +3.9‰, which belongs to control point 2640 in May 2014 and represents the lower range of $\delta^{18}O_{NO3}$ derived from nitrification. Some samples from Group 3 (sites 2554, 2640 and 2642) showed denitrification percentages up to 72% (site 2642 in September 2013, concurring with the lowest NO_3^- measured at this site). Denitrification reached similar percentages (up to 66% in site 2571) for Group 4 samples. For these samples, maximum denitrification rates were coupled to minimum NO_3^- concentrations (July-2015). The second assumed initial composition (s2 in Figure 5) had a $\delta^{15}N_{NO3}$ = +6.8‰ and a $\delta^{18}O_{NO3}$ = +6.6‰, representing approximately the upper range of $\delta^{18}O_{NO3}$ derived from nitrification. Several samples from sites 2571, 2602, 2640 and 2642 (n=14) clearly fit the denitrification trend starting from s2.

Considering samples from groups 3 and 4, with $\delta^{18}O_{NO3}$ values above +8.0‰ (n=50), the percentage of denitrification reached up to 72% in Group 3 (site 2642) and up to 60% in Group 4 (site 2571), together with lowest measured NO_3^- concentrations. Samples of sites 2554 and 2642 did not fit the expected denitrification trends, fitting to a lower ε_N:ε_O denitrification slope, closer to 2:1. Such a lower slope has been described in several field studies on denitrification (e.g. Böttcher et al., 1990). Potential explanations for the discrepancy between the slope obtained in the batch experiments and the slope at field scale include mixing processes with wastewater or manure sources, or the presence of NO_2^- re-oxidation processes (Wunderlich et al., 2013). During denitrification, NO_2^- is formed as an intermediate species, and can be quickly re-oxidized to NO_3^- incorporating atoms of oxygen from ambient water, thus lowering $\delta^{18}O_{NO3}$. Consistent with the literature, turnover of oxygen influences global biogeochemical processes, including the nitrogen cycle (Mader et al., 2017).

615 Denitrification can also be responsible for the absence of NO_3^- in lake water.
616 Nonetheless, the existence of other nitrate reduction processes, such as DNRA,
617 cannot be discarded at the water-sediment interface of Pétrola Lake. At 5 cm
618 depth, the lake sediment C:N ratios were between 4.4 and 57.3, and LOI
619 peaked at 19.0% (Appendix C). These results are consistent with previous
620 research, which found DNRA dominance in estuarine sediments with C:N ratios
621 of up to 10.6 (Dong et al., 2011). Song et al. (2013) showed that DNRA coexists
622 with denitrification and anammox in marine top sediments, with lower average
623 LOI (%) values (between 3.6% and 6.2%) than found in our study. The large
624 variability in lake sediment C:N ratios and LOI (%) was due to different sampling
625 locations within the lake. Considerable concentrations of NH_4^+ were measured
626 in groundwater below the lake (Gómez-Alday et al., 2014). These
627 concentrations of NH_4^+ can be related to DNRA in the water-sediment interface,
628 which are then further transported into the sediment, but also to other potential
629 sources of NH_4^+ described above (lake´s organic matter mineralization and
630 ammonium fertilizers). Even though conditions are favorable for DNRA, this
631 process could neither be confirmed nor rejected. Further research should be
632 undertaken to investigate these reactions by measuring the isotopic
633 composition of other N-compounds such as NH_4^+, NO_2^- or dissolved organic
634 nitrogen (Davidson et al., 2003).

635

636 ***5.4. Role of organic matter oxidation***

637 Previous studies showed the potential of organic matter present in PEB as the
638 main electron donor to promote denitrification and DNRA (Carrey et al., 2014a,
639 b; Gómez-Alday et al., 2014). Most of the $^{13}C_{DIC}$ values fall above the range of

640 groundwater $\delta^{13}C_{DIC}$ (between -11‰ and -15‰; Vogel and Ehhalt, 1963)
641 (Figure 6). These samples plotted far from fertilizers, considered to range
642 between -30‰ and -24‰ (Vitòria et al., 2004), and far from the mean isotopic
643 value for organic matter (-25‰; Hoefs, 1997).

644 Isotope data cannot explain the use of DOC for NO_3^- reduction because these
645 processes would increase HCO_3^- and decrease $\delta^{13}C_{DIC}$. Since part of the
646 aquifer is formed of Aptian carbonates, a possible explanation for the lack of a
647 clear correlation may be carbonate dissolution, which would increase the HCO_3^-
648 concentration. Anaerobic processes (e.g. denitrification) can trigger the
649 acidification of the solution, promoting such dissolution (Aravena and
650 Robertson, 1998; Krumins et al., 2013). Therefore, samples from the
651 surrounding area seem to be buffered by the aquifer materials and no insights
652 into this process can be gained using $\delta^{13}C_{DIC}$.

653 ---------- Fig. 6 near here ----------

654 Regarding lake water samples, $\delta^{13}C_{DIC}$ ranged from -16.3‰ to -4.8‰ (Figure 6).
655 Most of the samples showed $\delta^{13}C_{DIC}$ values close to the reference value of -8‰
656 for atmospheric CO_2 given by Clark and Fritz (1997). This probably reflects
657 degassing and CO_2 exchange with the atmosphere. Moreover, the ^{13}C
658 enrichment can also be a consequence of discrimination during photosynthesis
659 (Boutton, 1991). Samples with lower $\delta^{13}C_{DIC}$ matched up with high DOC and
660 low O_2 concentrations (<4.0 mgO_2/L). Organic matter oxidation with dissolved
661 O_2 and other electron acceptors (NO_3^- or SO_4^{2-}) in surface waters can shift the
662 $\delta^{13}C_{DIC}$ to values close to organic C ($\delta^{13}C_{org}$=-25‰). Nonetheless, this organic
663 matter oxidation should produce a decrease in DOC. On the contrary, DOC

664 increased in those samples with high EC, and hence this increase can be
665 related to the evaporation of the lake water.

666

667 ***6. Conclusions***

668 The current study was designed to identify the unusual ways of nitrogen
669 removal in a lake-aquifer interface by studying the hydrogeochemical and
670 isotopic evolution of a highly saline lake. The results showed that the underlying
671 aquifer is influenced by the Pétrola Lake and by the anthropogenic activities at
672 the basin scale. The multi-isotopic approach demonstrated that the origin of
673 NO_3^- in the lake aquifer-system was mainly related to synthetic ammonium
674 fertilizer applied in the agricultural areas of the basin, but also to the wastewater
675 inputs into the lake.

676 Denitrification was identified in the surrounding area of the lake, with similar
677 rates in dryland farming areas (up to 72%) and irrigation areas (up to 66%).
678 Denitrification in Pétrola basin is related with organic carbon oxidation. The ERT
679 demonstrated that DDF transported solutes from Pétrola Lake to the underlying
680 aquifer. These solutes are used by the microbial community at the freshwater-
681 saltwater interface. Nevertheless, the geometry of the freshwater-saltwater
682 interface is strongly influenced by land use. As a consequence of this variability,
683 reducing conditions were more marked in irrigation areas. Regarding lake
684 water, mineralization and organic matter degradation of lake sediment
685 apparently play a relevant role in nitrate reduction. In order to clarify the
686 microbial pathways of NO_3^- attenuation at the water-sediment interface, further
687 research should be undertaken by combining isotope techniques (e.g. isotope
688 pairing) with molecular biology tools.

689 Our results highlight the importance of freshwater-saltwater interfaces as
690 reactive zones for NO_3^- attenuation. In saline systems, the interaction between
691 density-driven down flow (DDF) and regional groundwater flow (RGF) is
692 influenced by anthropogenic activities. Thus, we underline the necessity of
693 including a land use perspective when studying water quality-environmental
694 relationships in systems dominated by density-driven circulation around the
695 world. Further studies should focus on the capacity of these interfaces to
696 remove other agricultural pollutants (i.e. pesticides), but also on the potential of
697 water-sediment interfaces to attenuate pollutants.

698

699 ***Acknowledgments***

700 This work was financed by a PhD grant (BES-2012-052256) from the Spanish
701 government, the PEIC-2014-004-P project from the Castilla–La Mancha
702 regional government, the projects CICYT CGL2014-57215-C4-1-R, CGL2017-
703 87216-C4-1-R and CGL2017-87216-C4-2-R from the Spanish Ministry of
704 Economy and AEU/FEDER UE, and the project 2017SGR1733 from the
705 Generalitat de Catalunya. The authors thank Michael Stachowitsch for the
706 English copyediting and valuable comments, as well as the Scientific and
707 Technological Centers of the University of Barcelona, the National Museum of
708 Natural History of the Spanish National Research Council, and the University of
709 Vienna for chemical and isotope analyses. We thank the anonymous reviewers
710 for their careful reading of the manuscript and their insightful comments.

711

712 ***References***

713 Andersen, M. S., Nyvang, V., Jakobsen, R., Postma, D. (2005). Geochemical
714 processes and solute transport at the seawater/freshwater interface of a sandy
715 aquifer. *Geochimica et Cosmochimica Acta*, *69*(16), 3979-3994.
716 https://doi.org/10.1016/j.gca.2005.03.017

717 APHA-AWWA-WEF (1998). Standard methods for the examination of water and
718 wastewater. Washington, DC: American Public Health Association, 1268.

719 Aravena, R., Robertson, W. D. (1998). Use of multiple isotope tracers to
720 evaluate denitrification in ground water: study of nitrate from a large-flux septic
721 system plume. *Ground Water*, *36*(6), 975-982. https://doi.org/10.1111/j.1745-
722 6584.1998.tb02104.x

723 Aravena, R., Mayer, B. (2009). Isotopes and processes in the nitrogen and
724 sulfur cycles. *Environmental isotopes in biodegradation and bioremediation*,
725 203-246.

726 Avrahamov, N., Antler, G., Yechieli, Y., Gavrieli, I., Joye, S. B., Saxton, M.,
727 Turchyn, A. V., Sivan, O. (2014). Anaerobic oxidation of methane by sulfate in
728 hypersaline groundwater of the Dead Sea aquifer. *Geobiology*, *12*(6), 511-528.
729 https://doi.org/10.1111/gbi.12095

730 Bernasconi, S. M., Barbieri, A., Simona, M. (1997). Carbon and nitrogen isotope
731 variations in sedimenting organic matter in Lake Lugano. *Limnology and*
732 *Oceanography*, *42*(8), 1755-1765. https://doi.org/10.4319/lo.1997.42.8.1755

733 Botrel, M., Gregory-Eaves, I., Maranger, R. (2014). Defining drivers of nitrogen
734 stable isotopes (δ15N) of surface sediments in temperate lakes. *Journal of*
735 *paleolimnology*, *52*(4), 419-433. https://doi.org/10.1007/s10933-014-9802-6

736 Böttcher, J., Strebel, O., Voerkelius, S., Schmidt, H. L. (1990). Using isotope
737 fractionation of nitrate-nitrogen and nitrate-oxygen for evaluation of microbial
738 denitrification in a sandy aquifer. *Journal of Hydrology*, *114*(3-4), 413-424.
739 https://doi.org/10.1016/0022-1694(90)90068-9

740 Boutton, T. W. (1991). Stable carbon isotope ratios of natural materials: II.
741 Atmospheric, terrestrial, marine, and freshwater environments. *Carbon isotope*
742 *techniques*, *1*, 173.

743 Brunet, R. C., Garcia-Gil, L. J. (1996). Sulfide-induced dissimilatory nitrate
744 reduction to ammonia in anaerobic freshwater sediments. *FEMS Microbiology*
745 *Ecology*, *21*(2), 131-138. https://doi.org/10.1016/0168-6496(96)00051-7

746 Burgin, A. J., Hamilton, S. K. (2007). Have we overemphasized the role of
747 denitrification in aquatic ecosystems? A review of nitrate removal
748 pathways. *Frontiers in Ecology and the Environment*, *5*(2), 89-96.
749 https://doi.org/10.1890/1540-9295(2007)5[89:HWOTRO]2.0.CO;2

750 Carrey, R., Otero, N., Soler, A., Gómez-Alday, J. J., Ayora, C. (2013). The role
751 of Lower Cretaceous sediments in groundwater nitrate attenuation in central
752 Spain: Column experiments. *Applied geochemistry*, *32*, 142-152.
753 https://doi.org/10.1016/j.apgeochem.2012.10.009

754 Carrey, R., Rodríguez-Escales, P., Otero, N., Ayora, C., Soler, A., Gómez-
755 Alday, J. J. (2014a). Nitrate attenuation potential of hypersaline lake sediments
756 in central Spain: Flow-through and batch experiments. *Journal of contaminant*
757 *hydrology*, *164*, 323-337. https://doi.org/10.1016/j.jconhyd.2014.06.017

758 Carrey, R., Otero, N., Vidal-Gavilan, G., Ayora, C., Soler, A., Gómez-Alday, J. J.
759 (2014b). Induced nitrate attenuation by glucose in groundwater: Flow-through

760 experiment. *Chemical Geology*, *370*, 19-28.
761 https://doi.org/10.1016/j.chemgeo.2014.01.016

762 Cartwright, I., Hall, S., Tweed, S., Leblanc, M. (2009). Geochemical and isotopic
763 constraints on the interaction between saline lakes and groundwater in
764 southeast Australia. *Hydrogeology journal*, *17*(8), 1991.
765 https://doi.org/10.1007/s10040-009-0492-5

766 Caschetto, M., Colombani, N., Mastrocicco, M., Petitta, M., Aravena, R. (2017).
767 Nitrogen and sulphur cycling in the saline coastal aquifer of Ferrara, Italy. A
768 multi-isotope approach. *Applied Geochemistry*, *76*, 88-98.
769 https://doi.org/10.1016/j.apgeochem.2016.11.014

770 Castanier, S., Bernet-Rollande, M. C., Maurin, A., Perthuisot, J. P. (1993).
771 Effects of microbial activity on the hydrochemistry and sedimentology of Lake
772 Logipi, Kenya. In *Saline Lakes V* (pp. 99-112). Springer Netherlands.

773 Cirujano, S., Montes, C., García, L. (1988). Los humedales de la provincia de
774 Albacete: una panorámica general. *Al-Basit: Revista de estudios albacetenses*,
775 (24), 77-95.

776 Clark, I. D., Fritz, P. (1997). *Environmental isotopes in hydrogeology*. CRC
777 press.

778 Colombani, N., Mastrocicco, M., Prommer, H., Sbarbati, C., Petitta, M. (2015).
779 Fate of arsenic, phosphate and ammonium plumes in a coastal aquifer affected
780 by saltwater intrusion. *Journal of contaminant hydrology*, *179*, 116-131.
781 https://doi.org/10.1016/j.jconhyd.2015.06.003

782 Daesslé, L. W., Orozco, A., Struck, U., Camacho-Ibar, V. F., van Geldern, R.,
783 Santamaría-del-Ángel, E., Barth, J. A. C. (2017). Sources and sinks of nutrients

784 and organic carbon during the 2014 pulse flow of the Colorado River into
785 Mexico. *Ecological Engineering*, *106*, 799-808.
786 https://doi.org/10.1016/j.ecoleng.2016.02.018

787 Davidson, E. A., Chorover, J., Dail, D. B. (2003). A mechanism of abiotic
788 immobilization of nitrate in forest ecosystems: the ferrous wheel
789 hypothesis. *Global Change Biology*, *9*(2), 228-236.
790 https://doi.org/10.1046/j.1365-2486.2003.00592.x

791 deGroot-Hedlin, C., Constable, S. (1990). Occam's inversion to generate
792 smooth, two-dimensional models from magnetotelluric
793 data. *Geophysics*, *55*(12), 1613-1624. https://doi.org/10.1190/1.1442813

794 Dong, L. F., Sobey, M. N., Smith, C. J., Rusmana, I., Phillips, W., Stott, A.,
795 Osborn, A. M., Nedwell, D. B. (2011). Dissimilatory reduction of nitrate to
796 ammonium, not denitrification or anammox, dominates benthic nitrate reduction
797 in tropical estuaries. *Limnology and Oceanography*, *56*(1), 279-291.
798 https://doi.org/10.4319/lo.2011.56.1.0279

799 Epstein, S., Mayeda, T. (1953). Variation of O18 content of waters from natural
800 sources. *Geochimica et cosmochimica acta*, *4*(5), 213-224.
801 https://doi.org/10.1016/0016-7037(53)90051-9

802 Eugster, H. P., Hardie, L. A. (1978). Saline lakes. In *Lakes* (pp. 237-293).
803 Springer New York.

804 Fraser, P. (1981). Health aspects of nitrate in drinking water. *Studies in*
805 *Environmental Science*, *12*, 103-116. https://doi.org/10.1016/S0166-
806 1116(08)70842-2

807 Gómez-Alday, J. J., Carrey, R., Valiente, N., Otero, N., Soler, A., Ayora, C.,
808 Sanz, D., Muñoz-Martin, A., Castaño, S., Recio, C., Carnicero, A., Cortijo, A.
809 (2014). Denitrification in a hypersaline lake–aquifer system (Pétrola Basin,
810 Central Spain): The role of recent organic matter and Cretaceous organic rich
811 sediments. *Science of the Total Environment*, *497*, 594-606.
812 https://doi.org/10.1016/j.scitotenv.2014.07.129

813 Gulis, G., Czompolyova, M., Cerhan, J. R. (2002). An ecologic study of nitrate in
814 municipal drinking water and cancer incidence in Trnava District,
815 Slovakia. *Environmental research*, *88*(3), 182-187.
816 https://doi.org/10.1006/enrs.2002.4331

817 Güler, C., Thyne, G. D. (2004). Hydrologic and geologic factors controlling
818 surface and groundwater chemistry in Indian Wells-Owens Valley area,
819 southeastern California, USA. *Journal of Hydrology*, *285*(1), 177-198.
820 https://doi.org/10.1016/j.jhydrol.2003.08.019

821 Hammer, U. T. 1981. Primary production in saline lakes, p. 47-57. In W. D.
822 Williams [eds.], Salt Lakes. Springer Netherlands.

823 Heaton, T. H. (1986). Isotopic studies of nitrogen pollution in the hydrosphere
824 and atmosphere: a review. *Chemical Geology: Isotope Geoscience Section*, *59*,
825 87-102. https://doi.org/10.1016/0168-9622(86)90059-X

826 Hill, A. R. (1996). Nitrate removal in stream riparian zones. *Journal of*
827 *environmental quality*, *25*(4), 743-755.
828 https://doi.org/10.2134/jeq1996.00472425002500040014x

829 Hodell, D. A., Schelske, C. L. (1998). Production, sedimentation, and isotopic
830 composition of organic matter in Lake Ontario. *Limnology and*
831 *Oceanography*, *43*(2), 200-214. https://doi.org/10.4319/lo.1998.43.2.0200

832 Hoefs, J. (1997). *Stable isotope geochemistry* (Vol. 201). Berlin: springer.

833 Horibe, Y., Shigehara, K., Takakuwa, Y. (1973). Isotope separation factor of
834 carbon dioxide-water system and isotopic composition of atmospheric
835 oxygen. *Journal of Geophysical Research*, *78*(15), 2625-2629.
836 https://doi.org/10.1029/JC078i015p0262

837 Hosono, T., Tokunaga, T., Tsushima, A., Shimada, J. (2014). Combined use of
838 δ 13 C, δ 15 N, and δ 34 S tracers to study anaerobic bacterial processes in
839 groundwater flow systems. *Water research*, *54*, 284-296.
840 https://doi.org/10.1016/j.watres.2014.02.005

841 ITAP. (2010). Datos sobre resultados de ensayos de cultivos [online]. Instituto
842 Técnico Agronómico y Provincial de Albacete.

843 Jetten, M. S., Strous, M., Van de Pas-Schoonen, K. T., Schalk, J., van Dongen,
844 U. G., van de Graaf, A. A., Logemann, S., Muyzer, G., van Loosdrecht, M. C.
845 M., Kuenen, J. G. (1998). The anaerobic oxidation of ammonium. *FEMS*
846 *Microbiology reviews*, *22*(5), 421-437. https://doi.org/10.1111/j.1574-
847 6976.1998.tb00379.x

848 Jones, B. F., Deocampo, D. M. (2003). Geochemistry of saline lakes. *Treatise*
849 *on geochemistry*, *5*, 605.

850 Jurado, A., Vàzquez-Suñé, E., Soler, A., Tubau, I., Carrera, J., Pujades, E.,
851 Anson, I. (2013). Application of multi-isotope data (O, D, C and S) to quantify

redox processes in urban groundwater. *Applied geochemistry*, *34*, 114-125. https://doi.org/10.1016/j.apgeochem.2013.02.018

Kelso, B., Smith, R. V., Laughlin, R. J., Lennox, S. D. (1997). Dissimilatory nitrate reduction in anaerobic sediments leading to river nitrite accumulation. *Applied and Environmental Microbiology*, *63*(12), 4679-4685.

Kendall, C., Elliott, E. M., Wankel, S. D. (2007). Tracing anthropogenic inputs of nitrogen to ecosystems. *Stable isotopes in ecology and environmental science*, *2*, 375-449.

Koroleff, F. (1969). Direct determination of ammonia in natural waters as indophenol blue. *ICES, CM*, *100*, 9.

Korom, S. F. (1992). Natural denitrification in the saturated zone: a review. *Water resources research*, *28*(6), 1657-1668. https://doi.org/10.1029/92WR00252

Kraft, B., Strous, M., Tegetmeyer, H. E. (2011). Microbial nitrate respiration–genes, enzymes and environmental distribution. *Journal of biotechnology*, *155*(1), 104-117. https://doi.org/10.1016/j.jbiotec.2010.12.025

Krumins, V., Gehlen, M., Arndt, S., Van Cappellen, P., Regnier, P. (2013). Dissolved inorganic carbon and alkalinity fluxes from coastal marine sediments: model estimates for different shelf environments and sensitivity to global change. *Biogeosciences*, *10*(1), 371-398. https://doi.org/10.5194/bg-10-371-2013

Lehmann, M. F., Bernasconi, S. M., Barbieri, A., McKenzie, J. A. (2002). Preservation of organic matter and alteration of its carbon and nitrogen isotope composition during simulated and in situ early sedimentary

diagenesis. *Geochimica et Cosmochimica Acta*, *66*(20), 3573-3584. https://doi.org/10.1016/S0016-7037(02)00968-7

Loke, M. H., Barker, R. D. (1996). Rapid least-squares inversion of apparent resistivity pseudosections by a quasi-Newton method. *Geophysical prospecting*, *44*(1), 131-152. https://doi.org/10.1111/j.1365-2478.1996.tb00142.x

Loke, M. H., Dahlin, T. (2002). A comparison of the Gauss–Newton and quasi-Newton methods in resistivity imaging inversion. *Journal of Applied Geophysics*, *49*(3), 149-162. https://doi.org/10.1016/S0926-9851(01)00106-9

Mader, M., Schmidt, C., van Geldern, R., Barth, J. A. (2017). Dissolved oxygen in water and its stable isotope effects: A review. *Chemical Geology*, *473,* 10-21. https://doi.org/10.1016/j.chemgeo.2017.10.003

Mayer, B., Bollwerk, S. M., Mansfeldt, T., Hütter, B., Veizer, J. (2001). The oxygen isotope composition of nitrate generated by nitrification in acid forest floors. *Geochimica et Cosmochimica Acta*, *65*(16), 2743-2756. https://doi.org/10.1016/S0016-7037(01)00612-3

McCready, R. G. L., Gould, W. D., Barendregt, R. W. (1983). Nitrogen isotope fractionation during the reduction of NO3− to NH4+ by Desulfovibrio sp. *Canadian Journal of Microbiology*, *29*(2), 231-234. https://doi.org/10.1139/m83-038

McIlvin, M. R., Altabet, M. A. (2005). Chemical conversion of nitrate and nitrite to nitrous oxide for nitrogen and oxygen isotopic analysis in freshwater and

seawater. *Analytical Chemistry*, *77*(17), 5589-5595. https://doi.org/10.1021/ac050528s

Mengis, M., Walther, U., Bernasconi, S. M., Wehrli, B. (2001). Limitations of using δ18O for the source identification of nitrate in agricultural soils. *Environmental science & technology*, *35*(9), 1840-1844. https://doi.org/10.1021/es0001815

Nelson, D.W., Sommers, L.E. (1996). Total Carbon, Organic Carbon, and Organic Matter. In *Methods of Soil Analysis. Part 3.* Soil Science Society of America and American Society of Agronomy, Madison, WI, USA, pp. 961–983

Orozco-Durán, A., Daesslé, L. W., Camacho-Ibar, V. F., Ortiz-Campos, E., Barth, J. A. C. (2015). Turnover and release of P-, N-, Si-nutrients in the Mexicali Valley (Mexico): Interactions between the lower Colorado River and adjacent ground-and surface water systems. *Science of the Total Environment*, *512*, 185-193. https://doi.org/10.1016/j.scitotenv.2015.01.016

Postma, D., Boesen, C., Kristiansen, H., Larsen, F. (1991). Nitrate reduction in an unconfined sandy aquifer: water chemistry, reduction processes, and geochemical modeling. *Water Resources Research*, *27*(8), 2027-2045.

Postma, D., Jakobsen, R. (1996). Redox zonation: equilibrium constraints on the Fe (III)/SO4-reduction interface. *Geochimica et Cosmochimica Acta*, *60*(17), 3169-3175. https://doi.org/10.1029/91WR00989

Puig, R., Folch, A., Menció, A., Soler, A., Mas-Pla, J. (2013). Multi-isotopic study (15 N, 34 S, 18 O, 13 C) to identify processes affecting nitrate and sulfate in response to local and regional groundwater mixing in a large-scale flow

923 system. *Applied geochemistry*, *32*, 129-141.
924 https://doi.org/10.1016/j.apgeochem.2012.10.014

925 Puig, R., Soler, A., Widory, D., Mas-Pla, J., Domènech, C., Otero, N. (2016).
926 Characterizing sources and natural attenuation of nitrate contamination in the
927 Baix Ter aquifer system (NE Spain) using a multi-isotope approach. *Science of*
928 *The Total Environment, 580,* 518-532.
929 https://doi.org/10.1016/j.scitotenv.2016.11.206

930 Rivett, M. O., Buss, S. R., Morgan, P., Smith, J. W., Bemment, C. D. (2008).
931 Nitrate attenuation in groundwater: a review of biogeochemical controlling
932 processes. *Water Research*, *42*(16), 4215-4232.

933 https://doi.org/10.1016/j.watres.2008.07.020

934 Ryabenko, E., Altabet, M. A., Wallace, D. W. (2009). Effect of chloride on the
935 chemical conversion of nitrate to nitrous oxide for δ15N analysis. *Limnology and*
936 *Oceanography: Methods*, *7*(7), 545-552. https://doi.org/10.4319/lom.2009.7.545

937 Ryther, J. H., Dunstan, W. M. (1971). Nitrogen, phosphorus, and eutrophication
938 in the coastal marine environment. *Science*, *171*(3975), 1008-1013.
939 https://doi.org/10.1126/science.171.3975.1008

940 Santoro, A. E. (2010). Microbial nitrogen cycling at the saltwater–freshwater
941 interface. *Hydrogeology Journal*, *18*(1), 187-202.
942 https://doi.org/10.1007/s10040-009-0526-z

943 Santoyo, E., García, R., Abella, R., Aparicio, A., Verma, S. P. (2001). Capillary
944 electrophoresis for measuring major and trace anions in thermal water and
945 condensed-steam samples from hydrothermal springs and fumaroles. *Journal of*

946 *Chromatography A*, *920*(1), 325-332. https://doi.org/10.1016/S0021-
947 9673(01)00835-4

948 Saunders, D. L., & Kalff, J. (2001). Nitrogen retention in wetlands, lakes and
949 rivers. *Hydrobiologia*, *443*(1-3), 205-212.
950 https://doi.org/10.1023/A:1017506914063

951 Schütt, B. (1998). Reconstruction of Holocene paleoenvironments in the
952 endorheic basin of Laguna de Gallocanta, Central Spain by investigation of
953 mineralogical and geochemical characters from lacustrine sediments. *Journal of*
954 *Paleolimnology*, *20*(3), 217-234. https://doi.org/10.1023/A:1007924000636

955 Skidmore, M., Tranter, M., Tulaczyk, S., Lanoil, B. (2010). Hydrochemistry of ice
956 stream beds—evaporitic or microbial effects? *Hydrological Processes*, *24*(4),
957 517-523. https://doi.org/10.1002/hyp.7580

958 Smith, V. H. (1998). Cultural eutrophication of inland, estuarine, and coastal
959 waters. In *Successes, limitations, and frontiers in ecosystem science* (pp. 7-49).
960 Springer New York.

961 Song, G. D., Liu, S. M., Marchant, H., Kuypers, M. M. M., Lavik, G. (2013).
962 Anammox, denitrification and dissimilatory nitrate reduction to ammonium in the
963 East China Sea sediment. *Biogeosciences*, *10*(11), 6851.
964 https://doi.org/10.5194/bg-10-6851-2013

965 Soukup, T., Büttner, G., Feranec, J., Hazeu, G., Jaffrain, G., Jindrova, M.,
966 Kopecky, M., Orlitova, E. (2016). CORINE Land Cover 2012 (CLC2012):
967 Analysis and Assessment. In *European Landscape Dynamics* (pp. 93-99). CRC
968 Press.

969 Stumm, W., Morgan, J. J. (1981). Aquatic chemistry: an introduction
970 emphasizing chemical equilibria in natural waters. In *Aquatic chemistry: An*
971 *introduction emphasizing chemical equilibria in natural waters* (pp. 795-795).

972 Tiedje, J. M. (1982). Denitrification. *Methods of Soil Analysis. Part 2. Chemical*
973 *and Microbiological Properties*, 1011-1026.

974 Tiedje, J. M. (1988). Ecology of denitrification and dissimilatory nitrate reduction
975 to ammonium. *Biology of anaerobic microorganisms*, *717*, 179-244.

976 Trimmer, M., Nedwell, D. B., Sivyer, D. B., Malcolm, S. J. (1998). Nitrogen
977 fluxes through the lower estuary of the river Great Ouse, England: the role of
978 the bottom sediments. *Marine Ecology Progress Series*, *163*, 109-124.

979 Valiente, N., Menchen, A., Jirsa, F., Hein, T., Wanek, W., Gomez-Alday, J. J.
980 (2016, April). Natural attenuation processes of nitrate in a saline lake-aquifer
981 system: Pétrola Basin (Central Spain). In *EGU General Assembly Conference*
982 *Abstracts* (Vol. 18, p. 6240).

983 Valiente, N., Carrey, R., Otero, N., Gutiérrez-Villanueva, M.A., Soler, A., Sanz,
984 D., Castaño, S., Gómez-Alday, J.J. Tracing sulfate recycling in the hypersaline
985 Pétrola Lake (SE Spain): A combined isotopic and microbiological approach.
986 *Chemical Geology, 473,* 74-89. https://doi.org/10.1016/j.chemgeo.2017.10.024

987 van den Berg, E. M., Boleij, M., Kuenen, J. G., Kleerebezem, R., van
988 Loosdrecht, M. C. (2016). DNRA and Denitrification Coexist over a Broad
989 Range of Acetate/N-NO3− Ratios, in a Chemostat Enrichment Culture. *Frontiers*
990 *in Microbiology*, *7: 1842*. https://doi.org/10.3389/fmicb.2016.01842

991 Vitòria, L., Otero, N., Soler, A., Canals, À. (2004). Fertilizer characterization:
992 isotopic data (N, S, O, C, and Sr). *Environmental Science &*
993 *Technology*, *38*(12), 3254-3262. https://doi.org/10.1021/es0348187

994 Vitòria, L., Soler, A., Aravena, R., Canals, A. (2005). Multi-isotopic approach
995 (15N, 13C, 34S, 18O and D) for tracing agriculture contamination in
996 groundwater. In *Environmental Chemistry* (pp. 43-56). Springer Berlin
997 Heidelberg.

998 Vogel, J. C., Ehhalt, D. (1963). The use of the carbon isotopes in groundwater
999 studies. In Symposium on the Radioisotopes in Hydrology, March 5–9, Tokyo,
1000 Japan, 383-395. Vienna Austria: International Atomic Energy Agency.

1001 Weber, K. A., Urrutia, M. M., Churchill, P. F., Kukkadapu, R. K., Roden, E. E.
1002 (2006). Anaerobic redox cycling of iron by freshwater sediment
1003 microorganisms. *Environmental Microbiology*, *8*(1), 100-113.
1004 https://doi.org/10.1111/j.1462-2920.2005.00873.x

1005

1006 Williams, W. D. (1996). The largest, highest and lowest lakes of the world:
1007 saline lakes. *Verhandlungen-Internationale Vereinigung für theoretische und*
1008 *angewandte Limnologie,* *26*: 61-79.
1009 https://doi.org/10.1080/03680770.1995.11900693

1010 Wood, E. D., Armstrong, F. A. J., Richards, F. A. (1967). Determination of
1011 nitrate in sea water by cadmium-copper reduction to nitrite. *Journal of the*
1012 *Marine Biological Association of the United Kingdom*, *47*(1), 23-31.

1013 Wood, W. W., Sanford, W. E. (1990). Ground-water control of evaporite
1014 deposition. *Economic Geology*, *85*(6), 1226-1235.
1015 https://doi.org/10.1017/S002531540003352X

1016 Wunderlich, A., Meckenstock, R. U., Einsiedl, F. (2013). A mixture of nitrite-
1017 oxidizing and denitrifying microorganisms affects the δ 18O of dissolved nitrate
1018 during anaerobic microbial denitrification depending on the δ18O of ambient
1019 water. *Geochimica et Cosmochimica Acta*, *119*, 31-45.
1020 https://doi.org/10.1016/j.gca.2013.05.028

1021 Yechieli, Y., Wood, W. W. (2002). Hydrogeologic processes in saline systems:
1022 playas, sabkhas, and saline lakes. *Earth-Science Reviews*, *58*(3), 343-365.
1023 https://doi.org/10.1016/S0012-8252(02)00067-3

1024

Figure1

Click here to download high resolution image

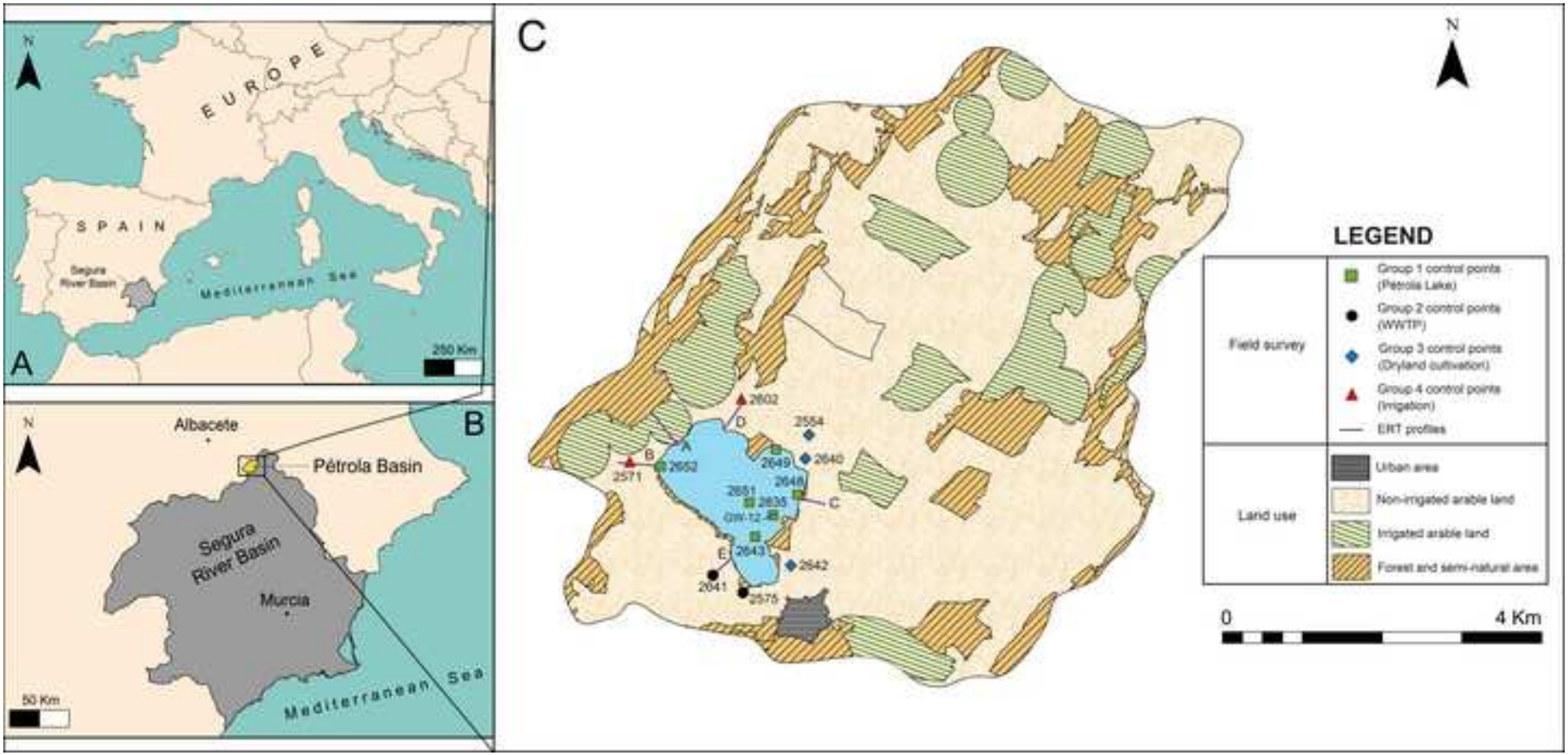

Figure2

Click here to download high resolution image

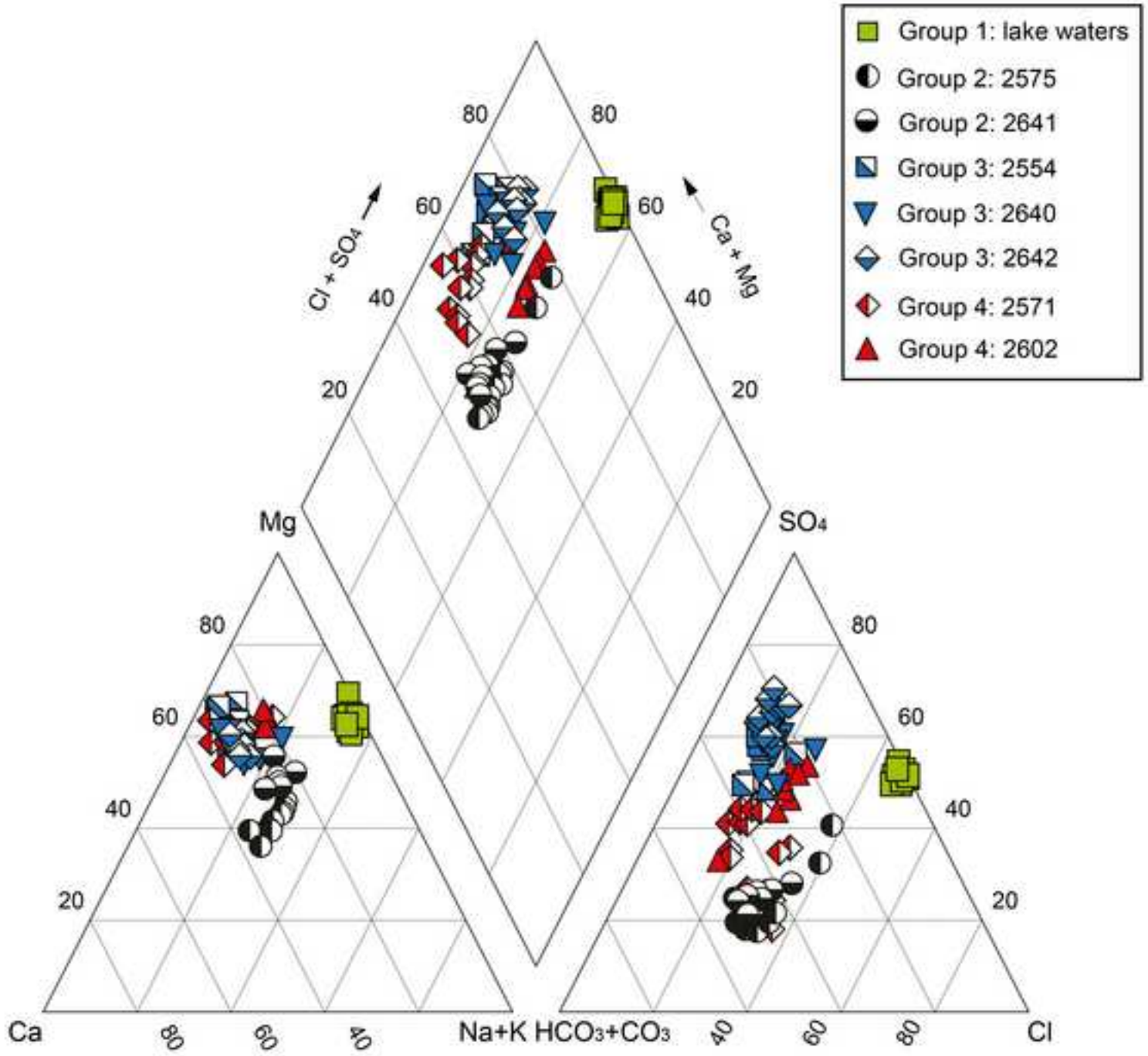

Figure3

Click here to download high resolution image

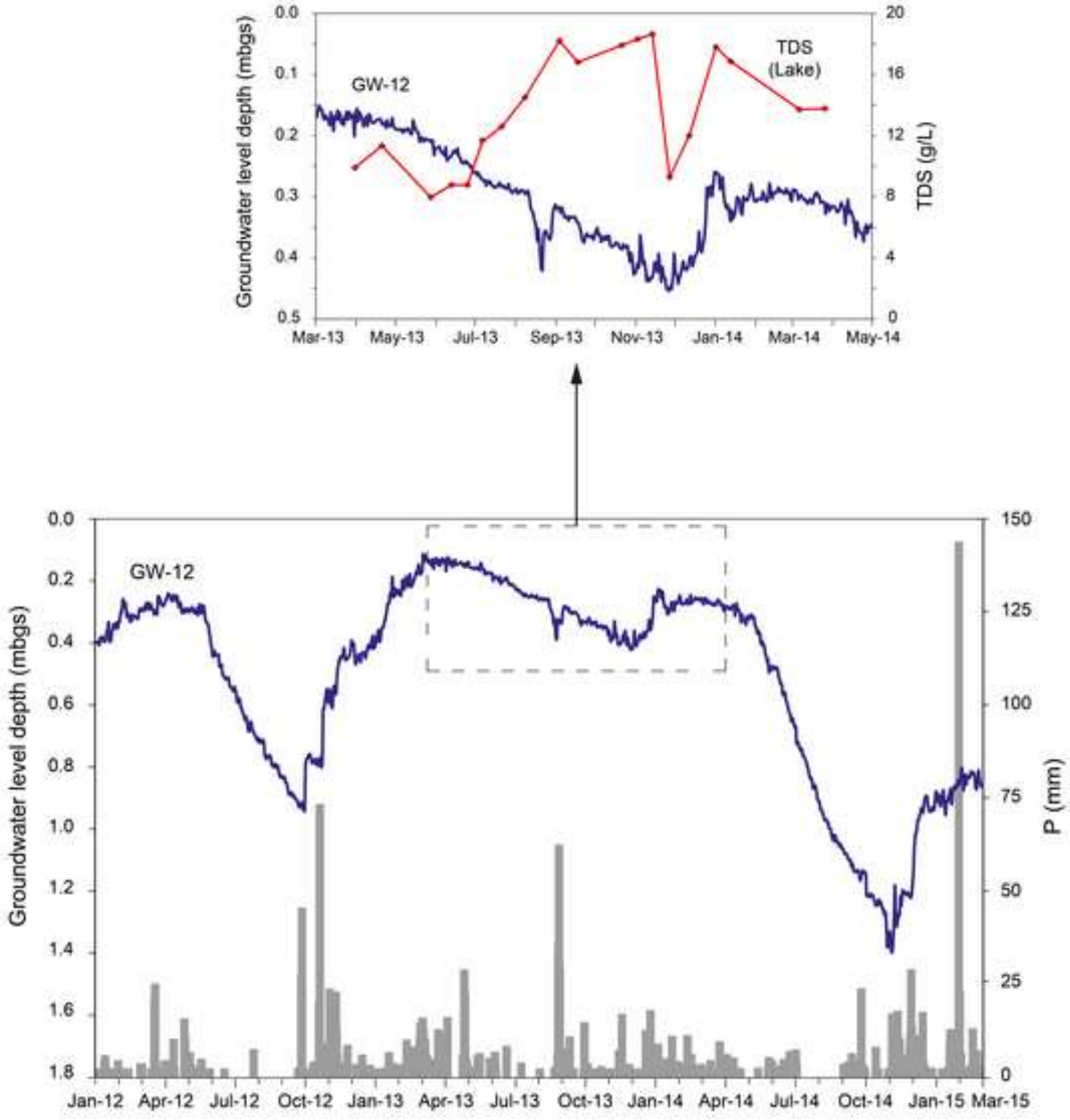

Figure4

Click here to download high resolution image

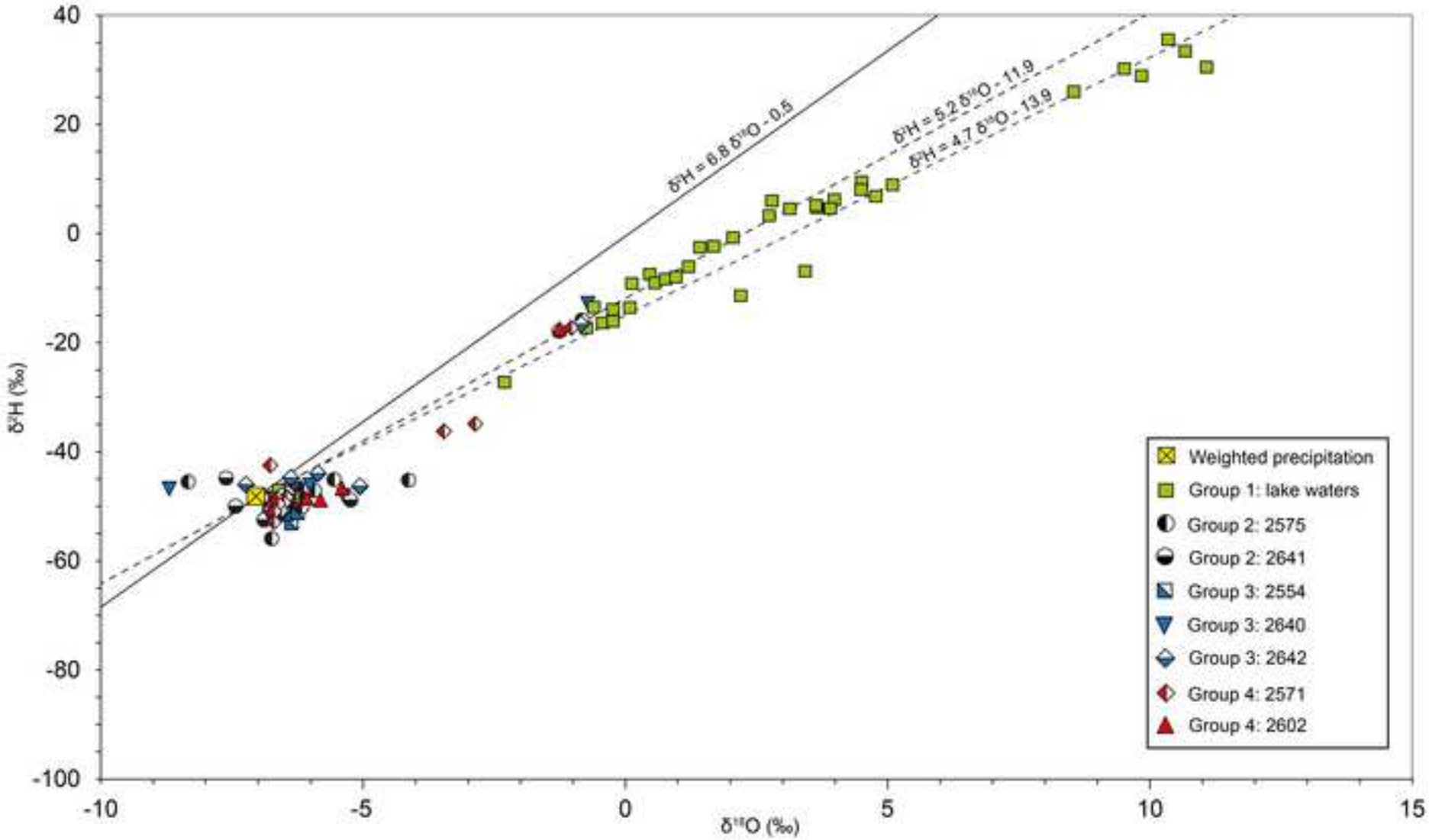

Figure5

Click here to download high resolution image

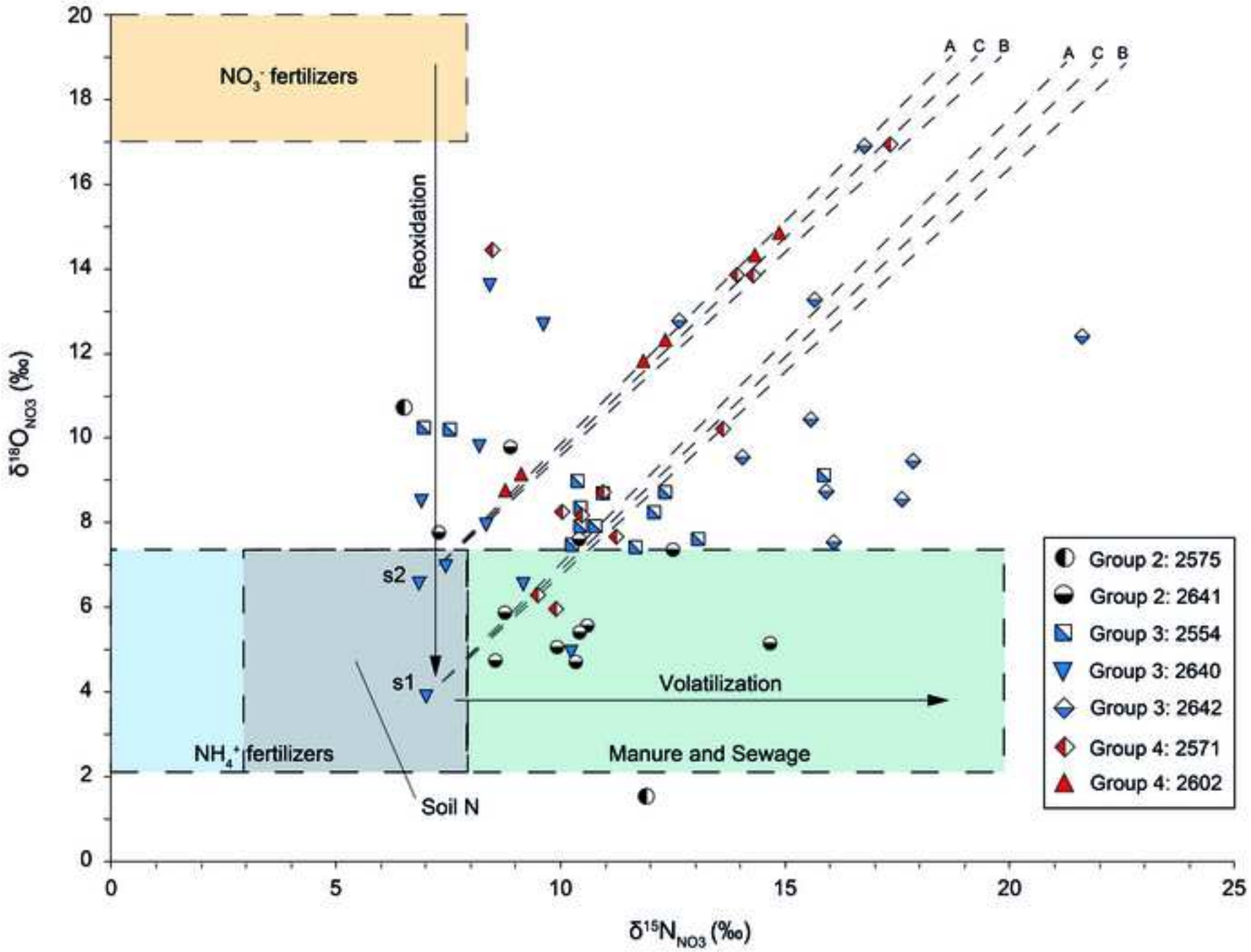

Figure6

Click here to download high resolution image

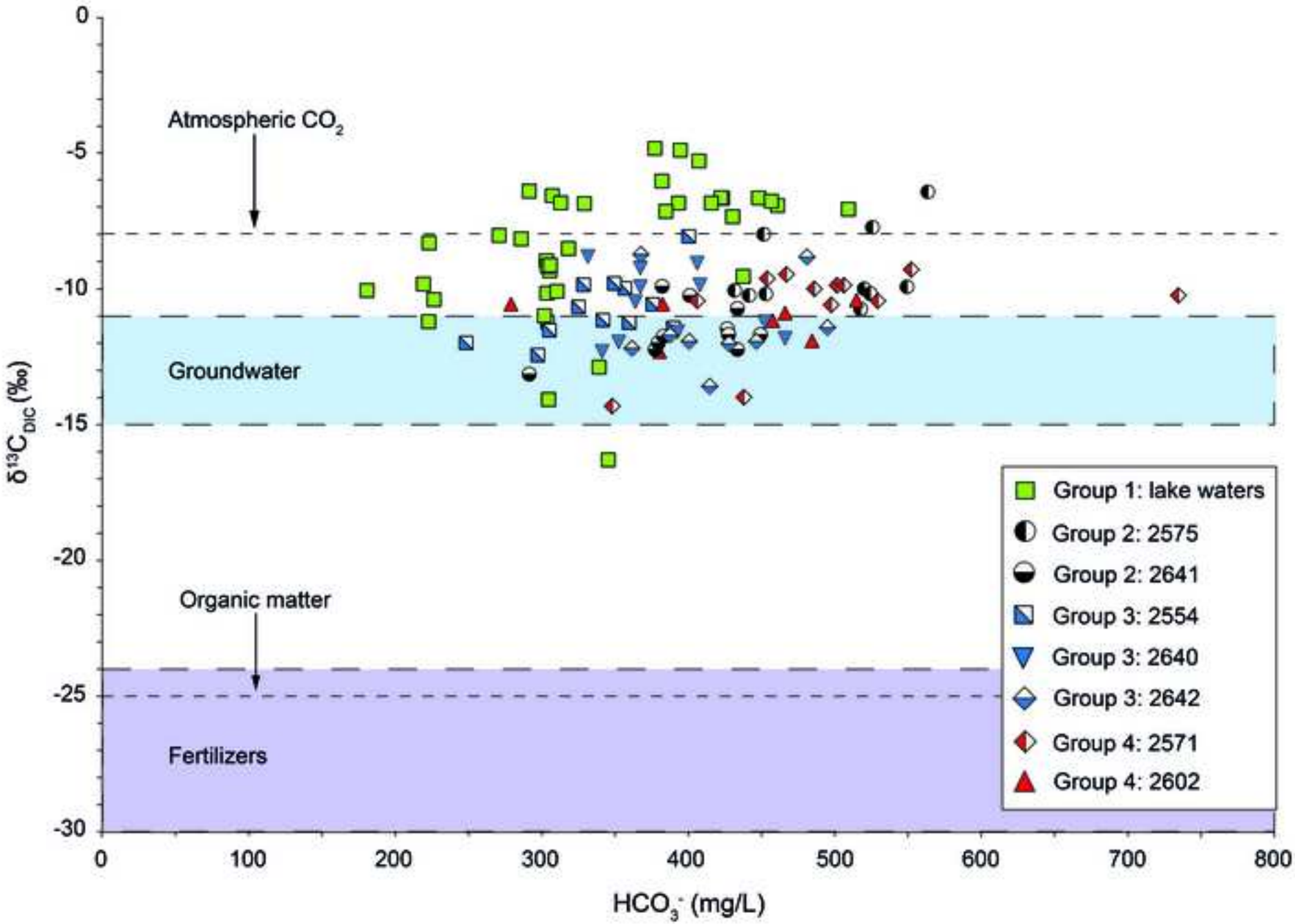

A multi-isotopic approach to investigate the influence of land use on nitrate removal in a highly saline lake-aquifer system

Figure captions

Figure	Caption
Figure 1.	A) Location of Segura River Basin in Europe. B) Location of Pétrola basin in Segura River Basin. C) Land use map of Pétrola basin and location of control points from Group 1 (Pétrola Lake, green squares), Group 2 (urban wastewater, black circles), Group 3 (dryland cultivation, blue rhombus), Group 4 (irrigated croplands, red triangles), and ERT profiles (A, B, C, D and E).
Figure 2.	Piper diagram showing the chemical composition of the water samples during the period 2013 to 2015.
Figure 3.	Groundwater depth (mbgs) in GW-12 and precipitation (P) between January 2012 and March 2015. In detail, groundwater depth evolution in GW-12 from March 2013 to May 2014 compared to mean TDS evolution in lake waters.
Figure 4.	$\delta^{18}O$ versus $\delta^{2}H$ plot including the weighted average precipitation of Madrid, water samples from Pétrola Lake (Group 1, n=40), and samples from the surrounding area (Groups 2, 3 and 4, n=79). Regression line 1 ($\delta^{2}H = 4.7\delta^{18}O - 13.9$) was calculated for lake water samples and compared with regression line 2 ($\delta^{2}H = 5.2\delta^{18}O - 11.9$) using water samples from piezometers and surface water in previous studies (n=29) collected between 2008 and 2010 (Valiente et al., 2017). Regression line 3 ($\delta^{2}H = 6.8\delta^{18}O - 0.5$) represents the Local Meteoric Water Line of Madrid.
Figure 5.	$\delta^{15}N$ and $\delta^{18}O$ of dissolved NO_3^- in the collected samples from the surrounding area (Groups 2, 3 and 4, n=63). The isotopic composition of the main NO_3^- sources is represented: ammonium fertilizers, nitrate fertilizers, soil N, and animal manure or sewage (Vitòria et al. 2004; Kendall et al., 2007; Aravena and Mayer, 2009; Puig et al., 2016). Dashed lines represent denitrification (%) using Utrillas sediments (A: ε_O= -12.1‰, ε_N= -11.6‰; B: ε_O=-13.8‰, ε_N= -15.7‰) and recent organic matter from hypersaline sediments (C: ε_O=-14.5‰; ε_N -14.7‰). s1 and s2 reflect the sources of dissolved NO_3^- used for denitrification % calculations.
Figure 6.	HCO_3^- and $\delta^{13}C_{DIC}$ analyzed in water samples from Pétrola Lake (Group 1, n=37), and samples from the surrounding area (Groups 2, 3 and 4, n=73). The isotopic compositions of atmospheric CO_2, groundwater, organic matter and fertilizers are represented (Vogel and Ehhalt, 1963; Clark and Fritz, 1997; Hoefs, 1997; Vitòria et al., 2004).

AppendixA

Click here to download Supplementary material for on-line publication only: AppendixA_Valiente_STOTEN-D-18-00612.pdf

AppendixB

Click here to download Supplementary material for on-line publication only: AppendixB_Valiente_STOTEN-D-18-00612.pdf

AppendixC

Click here to download Supplementary material for on-line publication only: AppendixC_Valiente_STOTEN-D-18-00612.pdf

AppendixD

Click here to download Supplementary material for on-line publication only: AppendixD_Valiente_STOTEN-D-18-00612.pdf